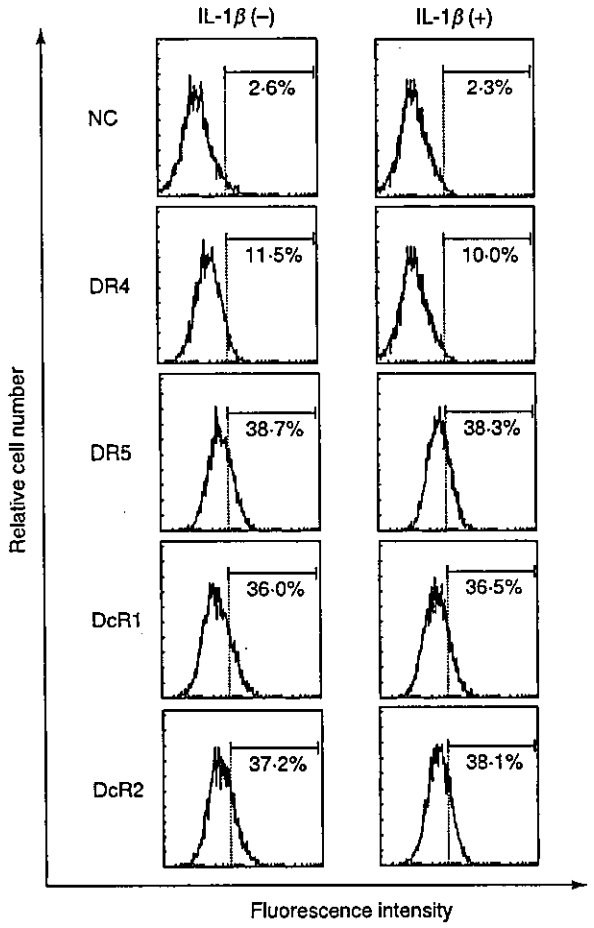

Fig. 6. IL-1β does not modulate the expression of DR4, DR5, DcR1 and DcR2 on FLS. Rheumatoid FLS, cultured in the presence or absence of rIL-1β (20 IU/ml) for 72 h, were detached by adding 0·265 mM EDTA and reacted with anti-DR4, anti-DR5, anti-DcR1 or anti-DcR2 at 4°C for 30 min. The cells were incubated further with PE-conjugated antigoat IgG at 4°C for 30 min, and surface expression of DR4, DR5, DcR1 and DcR2 on FLS was examined by flow cytometer as described in the text. Note that the expression of DR4, DR5, DcR1 and DcR2 on FLS was not changed by IL-1β treatment. NC: negative control, stained with goat IgG instead of first antibody. Numbers are the percentage of positive cells. Results are representative data from five individual samples.

induced apoptosis in FLS (see Figs 1 and 3). OPG protein concentration in rheumatoid synovial fluid reported by other groups [15,16,23] was much higher than the present data. Factors responsible for the difference are unclear; however, the variation in clinical situations of the subjects and MoAb used might result in the difference. Recent investigations have shown the elevation of OPG in rheumatoid synovial fluid, compared with serum consentration [15]; however, other investigators demonstrated a relatively low OPG protein concentration in the rheumatoid synovial fluid compared with synovial fluid from osteoarthritis patients [23]. Further investigation is necessary to clarify the functional expression of OPG in synovial tissue of RA patients.

TRAIL is thought to be an inhibitor of synovial cell hyperplasia as the blockage of TRAIL signalling by sDR5 in type II collagen-induced arthritis in mice exacerbates the proliferation of synovial cells [24]. Although we have not examined the expression of other soluble receptor antagonists such as sDR4 and sDR5 in the culture supernatants of FLS, our present study indicates that OPG produced by synovial cells acts as an endogenous decoy receptor of TRAIL-induced apoptosis, and part of the growth-promoting activity of IL-1β may be achieved by overproduction of OPG to suppress the biological function of TRAIL.

ACKNOWLEDGEMENT

This study was supported in part by grant-in-aid 13557042/13670461 from the Ministry of Education, Science, and Culture of Japan.

REFERENCES

1 Simonet WS, Lacey DL, Dunstan CR *et al.* Osteoprotegerin: a novel secreted protein involved in the regulation of bone density. Cell 1997; **89**:309–19.
2 Tsuda E, Goto M, Mochizuki S *et al.* Isolation of a novel cytokine from human fibroblasts that specifically inhibits osteoclastogenesis. Biochem Biophys Res Commun 1997; **234**:137–42.
3 Yasuda H, Shima N, Nakagawa N *et al.* Identity of osteoclastogenesis inhibitory factor (OCIF) and osteoprotegerin (OPG): a mechanism by which OPG/OCIF inhibits osteoclastogenesis *in vitro*. Endocrinology 1998; **139**:1329–37.
4 Tomoyasu A, Goto M, Fujise N *et al.* Characterization of monomeric and homodimeric forms of osteoclastogenesis inhibitory factor. Biochem Biophys Res Commun 1998; **245**:382–7.
5 Collin-Osdoby P, Rothe L, Anderson F, Nelson M, Maloney W, Osdoby P. Receptor activator of NF-κB and osteoprotegerin expression by human microvascular endothelial cells, regulation by inflammatory cytokines, and role in human osteoclastogenesis. J Biol Chem 2001; **276**:20659–72.
6 Kwon BS, Wang S, Udagawa N *et al.* TR1, a new member of the tumor necrosis factor receptor superfamily, induces fibroblast proliferation and inhibits osteoclastogenesis and bone resorption. FASEB J 1998; **12**:845–54.
7 Malyankar UM, Scatena M, Suchland KL *et al.* Osteoprotegerin is an $\alpha_v\beta_3$-induced, NF-$\acute{e}$B-dependent survival factor for endothelial cells. J Biol Chem 2000; **275**:20959–62.
8 Vaishnaw AK, McNally JD, Elkon KB. Apoptosis in the rheumatic diseases. Arthritis Rheum 1997; **40**:1917–27.
9 Kawakami A, Eguchi K, Matsuoka N *et al.* Inhibition of Fas antigen-mediated apoptosis of rheumatoid synovial cells *in vitro* by transforming growth factor beta 1. Arthritis Rheum 1996; **39**:1267–76.
10 Tsuboi M, Eguchi K, Kawakami A *et al.* Fas antigen expression on synovial cells was down-regulated by interleukin 1 beta. Biochem Biophys Res Commun 1996; **218**:280–5.
11 Kawakami A, Nakashima T, Yamasaki S *et al.* Regulation of synovial cell apoptosis by proteasome inhibitor. Arthritis Rheum 1999; **42**:2440–8.
12 Emery JG, McDonnell P, Burke MB *et al.* Osteoprotegerin is a receptor for the cytotoxic ligand TRAIL. J Biol Chem 1998; **273**:14363–7.
13 Miyashita T, Kawakami A, Tamai M *et al.* Akt is an endogenous inhibitor toward tumor necrosis factor-related apoptosis inducing ligand (TRAIL)-mediated apoptosis in rheumatoid synovial cells. Biochem Biophys Res Commun 2003; **312**:397–404.
14 Arnett FC, Edworthy SM, Bloch DA *et al.* The American Rheumatism Association 1987 revised criteria for the classification of rheumatoid arthritis. Arthritis Rheum 1998; **31**:315–24.
15 Feuerherm AJ, Borset M, Seidel C *et al.* Elevated levels of osteoprotegerin (OPG) and hepatocyte growth factor (HGF) in rheumatoid arthritis. Scand J Rheumatol 2001; **30**:229–34.
16 Ziolkowska M, Kurowska M, Radzikowska A *et al.* High levels of osteoprotegerin and soluble receptor activator of nuclear factor kappa B ligand in serum of rheumatoid arthritis patients and their normalization after anti-tumor necrosis factor alpha treatment. Arthritis Rheum 2002; **46**:1744–53.

17 Pan G, Ni J, Wei YF, Yu G, Gentz R, Dixit VM. An antagonist decoy receptor and a death domain-containing receptor for TRAIL. Science 1997; **277**:815–8.
18 Pan G, O'Rourke K, Chinnaiyan AM *et al.* The receptor for the cytotoxic ligand TRAIL. Science 1997; **276**:111–3.
19 Ichikawa K, Liu W, Fleck M *et al.* TRAIL-R2 (DR5) mediates apoptosis of synovial fibroblasts in rheumatoid arthritis. J Immunol 2003; **171**:1061–9.
20 Truneh A, Sharma S, Doyle ML *et al.* Temperature-sensitive differential affinity of TRAIL for its receptors. DR5 is the highest affinity receptor. J Biol Chem 2000; **275**:23319–25.
21 Duff GW. Cytokines and acute phase proteins in rheumatoid arthritis. Scand J Rheumatol 1994; **100**:9–19.
22 Kong YY, Feige U, Sarosi I *et al.* Activated T cells regulate bone loss and joint destruction in adjuvant arthritis through osteoprotegerin ligand. Nature 1999; **402**:304–9.
23 Kotake S, Udagawa N, Hakoda M, Tomatsu T, Suda T, Kamatani N. Activated human T cells directly induce osteoclastogenesis from human monocytes: possible role of T cells in bone destruction in rheumatoid arthritis patients. Arthritis Rheum 2001; **44**:1003–12.
24 Song K, Chen Y, Goke R *et al.* Tumor necrosis factor-related apoptosis-inducing ligand (TRAIL) is an inhibitor of autoimmune inflammation and cell cycle progression. J Exp Med 2000; **191**:1095–104.

Plasma Level of B-Type Natriuretic Peptide as a Prognostic Marker After Acute Myocardial Infarction

A Long-Term Follow-Up Analysis

Satoru Suzuki, MD; Michihiro Yoshimura, MD; Masafumi Nakayama, MD; Yuji Mizuno, MD; Eisaku Harada, MD; Teruhiko Ito, MD; Shota Nakamura, MD; Koji Abe, MD; Megumi Yamamuro, MD; Tomohiro Sakamoto, MD; Yoshihiko Saito, MD; Kazuwa Nakao, MD; Hirofumi Yasue, MD; Hisao Ogawa, MD

Background—Circulating levels of B-type natriuretic peptide (BNP), a cardiac hormone, reflect the severity of cardiac dysfunction. Because the plasma BNP level changes dramatically during the period after the onset of acute myocardial infarction (AMI), identification of a suitable sampling time is problematic. There have been several reports indicating that the plasma BNP level obtained in the acute phase of AMI can be used as a prognostic marker. We examined whether the plasma BNP level measured 3 to 4 weeks after the onset of AMI represents a reliable prognostic marker for patients with AMI.

Methods and Results—We analyzed 145 consecutive patients with AMI. Plasma BNP levels were measured during the 3 to 4 weeks after onset of AMI. Of those patients, 23 experienced fatal cardiac events during this study. The mean follow-up period was 58.6 months. Log BNP, left ventricular end-diastolic pressure, and pulmonary vascular resistance were all significantly higher in the cardiac death group, and there were more men and more patients with a history of heart failure in the cardiac death group. A Cox proportional hazards model analysis showed that log BNP was an independent predictor of cardiac death. The survival rate was significantly higher in patients with log BNP <2.26 (180 pg/mL) than in those with log BNP ≥ 2.26.

Conclusions—The plasma BNP level obtained 3 to 4 weeks after the onset of AMI can be used as an independent predictor of cardiac death in patients with AMI. (***Circulation.*** **2004;110:1387-1391.**)

Key Words: natriuretic peptides ■ myocardial infarction ■ prognosis

B-type natriuretic peptide (BNP) is a cardiac hormone that is secreted mainly from the ventricles; it has many biological effects, including vasodilation, natriuresis, and inhibition of both the rennin-angiotensin and sympathetic nervous systems.[1-7] BNP is secreted from the failing heart into the systemic circulation; the plasma level of this peptide is elevated in patients with heart failure.[8-11] The plasma BNP level has been recognized as a biochemical marker of ventricular dysfunction.[9-15]

We previously reported that the plasma BNP level increases rapidly and markedly just after the onset of acute myocardial infarction (AMI).[13,16] The plasma level of BNP changes dramatically in some patients. The time course of the plasma BNP level could be divided into 2 patterns after the onset of AMI: a biphasic pattern with 2 peaks and a monophasic pattern with 1 peak. There were significantly more patients with anterior infarction, congestive heart failure, a higher maximum level of creatine kinase-MB isoenzyme, and a lower left ventricular ejection fraction in the biphasic group than in the monophasic group; this suggests that the biphasic pattern reflects the degree of left ventricular dysfunction or the size of the infarct.[13]

The mechanism for the formation of the first plasma BNP peak was shown to be due to the genetic characteristics of BNP: The DNA of BNP has an AT-rich sequence in the 3′-untranslated region, which destabilizes mRNA.[12,17] For this reason, BNP is considered to be an acute-phase reactant in response to acute tissue injuries.[12,13,17,18] Hemodynamic parameters, as well as some humoral factors such as interleukin-1β, endothelin-1, and angiotensin II, induce secretion of BNP in the early phase of AMI, thus accounting for the first peak.[13,19-22] The mechanisms for the formation of the

Received January 16, 2004; de novo received March 30, 2004; revision received May 4, 2004; accepted May 6, 2004.

From the Department of Cardiovascular Medicine (S.S., M. Yoshimura, M.N., S.N., K.A., M. Yamamuro, T.S., H.O.), Graduate School of Medical Sciences, Kumamoto University, Kumamoto, Japan; Division of Cardiology (Y.M., E.H., T.I., H.Y.), Kumamoto Aging Research Institute, Kumamoto, Japan; First Department of Internal Medicine (Y.S.), Nara Medical University, Nara, Japan; and Department of Medicine and Clinical Science (K.N.), Kyoto University Graduate School of Medicine, Kyoto, Japan.

Reprint requests to Michihiro Yoshimura, Department of Cardiovascular Medicine, Graduate School of Medical Sciences, Kumamoto University, 1-1-1 Honjo, Kumamoto 860-8556, Japan. E-mail bnp@kumamoto-u.ac.jp

Circulation is available at http://www.circulationaha.org

DOI: 10.1161/01.CIR.0000141295.60857.30

second peak are considered to be related to infarct expansion and subsequent ventricular remodeling.[12,13]

As mentioned above, the changing pattern of the plasma BNP level varies according to the cardiac condition after AMI. This raises the possibility that the plasma BNP level could reflect or predict prognosis after the onset of AMI. The changing pattern of the plasma BNP level after the onset of AMI is dynamic during the first month; therefore, identification of a suitable time frame for blood sampling for BNP measurement is an important issue. To exploit the plasma BNP level as a clinically useful prognostic marker after AMI in the future, it would be convenient to measure it 3 to 4 weeks after the onset of AMI. It is generally difficult to target the timing of the blood sampling to the formation of the second plasma BNP peak, although this strict time point may be better as a prognostic marker than the later phase, such as 3 to 4 weeks after the onset. According to our previous study, the plasma BNP level was still significantly higher in patients with the biphasic pattern than in those with the monophasic pattern at 3 to 4 weeks after onset of AMI,[13] which suggests that sampling at this time would also be valuable for clinical use. In the present study, we examined whether the plasma BNP level measured 3 to 4 weeks after the onset of AMI represents a reliable prognostic marker after AMI by monitoring patients with AMI for a long-term period. The present study began just after the discovery of BNP, and therefore we were able to monitor the patients for ~5 years on average and as long as 13 years.

Methods

Study Patients

This study began in January 1990, just after the discovery of BNP, and an antibody for BNP was established by our research group.[9,23,24] The end of the patient recruitment period was in March 1999. The final follow-up date was on May 31, 2003. During this time period, there were 403 admitted patients with AMI who underwent cardiac catheterization and in whom we were able to measure the plasma BNP level 3 to 4 weeks after the onset of AMI. We followed up 285 patients and were ultimately able to follow up 145 patients with highly reliable information about their prognosis from themselves, their families, and/or their affiliated hospitals. The 145 study patients consisted of 106 men and 39 women with a mean age of 65.1 years (range 31 to 90 years).

The diagnosis of AMI was made from clinical symptoms, including chest pain, ECG changes including ST elevation and ST depression, and an elevation of serum creatine kinase-MB isoenzyme to more than twice the normal upper level. In the present study, we defined the cardiac death group as patients who died of heart failure or sudden cardiac death and the non–cardiac-death group as survivors, including patients who died of causes other than cardiac events. The protocol was in agreement with the guidelines of the ethics committee at our institution, and written informed consent was obtained from each patient before they were enrolled in the study.

Cardiac Catheterization

Cardiac catheterization was performed in 145 patients at 3 to 4 weeks after AMI. A Swan-Ganz catheter was inserted into the femoral or subclavian vein, and hemodynamic measurements were obtained, including pulmonary capillary wedge pressure, pulmonary artery pressure, right atrial pressure, and cardiac output. Cardiac output was determined in triplicate by the thermodilution technique. Blood samples that included BNP were obtained from either the femoral or subclavian vein.

After the Swan-Ganz catheterization procedure, aortic pressure and left ventricular end-diastolic pressure were measured; then, coronary angiography and left ventriculography were performed. The left ventricular ejection fraction was determined by left ventriculography.

Measurement of BNP Plasma Level

The plasma BNP concentration was measured with a specific radioimmunoassay for human BNP from 1990 to 1993[9,25,26] and then a specific immunoradiometric assay for human BNP from 1993 to 1999 (Shionoria BNP; Shionogi Inc).[27] There were no significant differences in the BNP values obtained by the radioimmunoassay and immunoradiometric assay methods.[28]

Statistical Analysis

Continuous values are expressed as the mean±SD. Statistical significance was defined as a probability value <0.05. A Cox proportional hazards regression analysis was performed to identify independent predictors of cardiac death by using variables including log BNP, left ventricular ejection fraction, history of heart failure, heart rate, male gender, anterior myocardial infarction, ACE inhibitor or β-blocker use, history of renal dysfunction, age, history of left ventricular hypertrophy, and revascularization. Because the BNP plasma level was not normally distributed, we selected log BNP for analysis. A log BNP cutoff point was selected to define a large patient group with a low risk of cardiac death. A Kaplan-Meier survival curve was used for survival comparisons between patient groups stratified according to this cutoff point.

Results

Follow-Up Periods

The mean follow-up period was 58.6 months (range 1 to 158 months) for all study patients, with mean follow-up periods of 41.3 months (range 1 to 127 months) for the cardiac death group and 61.9 months (range 1 to 158 months) for the non–cardiac-death group.

Prognosis of Patients and Causes of Death

Of the 145 patients, 115 survived and 30 died during the study period. Of the 30 patients who died, 8 (27%) died of sudden death, 15 (50%) had heart failure, and 7 (23%) died of other causes (2 of pneumonia, 2 of lung cancer, 1 of renal cell carcinoma, 1 of liver dysfunction, and 1 of blood dyscrasia).

Comparisons of Clinical Characteristics, Hemodynamic Parameters, and Plasma BNP Levels Between the Cardiac Death Group and the Non–Cardiac-Death Group

The clinical characteristics and hemodynamic parameters of the study patients are shown in Tables 1 and 2. Among all the patients, 72 (50%) had anterior infarction, and 73 (50%) had inferior or posterolateral infarction. Eighty-four (60%) had a history of smoking, 48 (35%) had a history of hypertension, 37 (27%) were obese, 62 (45%) had diabetes mellitus, and 57 (41%) had dyslipidemia (Table 1).

The number of male patients and patients with a history of heart failure was significantly higher in the cardiac death group than in the non–cardiac-death group. There were no significant differences for age, anterior myocardial infarction, coronary risk factors, history of left ventricular hypertrophy, history of renal dysfunction, revascularization, or pharmacotherapy between the cardiac death group and the non–cardiac-death group (Table 1).

TABLE 1. Patients' Characteristics

	Non–Cardiac-Death (n=122)	Cardiac Death (n=23)	P
Age, y	64.7±11.1	66.7±7.9	NS
Male gender	70 (85/122)	91 (21/23)	0.03
Anterior MI	47 (57/122)	65 (15/23)	NS
Smoking	60 (71/119)	65 (13/20)	NS
History of hypertension	37 (44/119)	20 (4/20)	NS
Obesity	28 (33/119)	20 (4/20)	NS
Diabetes mellitus	46 (55/119)	35 (7/20)	NS
History of dyslipidemia	44 (52/119)	25 (5/20)	NS
History of heart failure	4 (5/117)	18 (4/22)	0.015
History of LVH	17 (20/117)	5 (1/22)	NS
History of renal dysfunction	19 (19/102)	33 (6/18)	NS
Revascularization*	53 (62/116)	52 (11/21)	NS
Pharmacotherapy			
ACEI	45 (50/111)	45 (9/20)	NS
Digitalis	3 (3/111)	5 (1/20)	NS
Furosemide	17 (19/111)	25 (5/20)	NS
Spironolactone	3 (3/111)	5 (1/20)	NS
Calcium channel blocker	80 (88/111)	75 (15/20)	NS
Nitrate	59 (65/111)	60 (12/20)	NS
β-Blocker	20 (22/111)	30 (6/20)	NS

Values are percentage (number) of patients or mean±SD. Anterior MI indicates patients with anterior myocardial infarction; LVH, left ventricular hypertrophy.

*Including percutaneous coronary intervention, thrombolytic therapy, and CABG.

Log BNP was significantly higher in the cardiac death group than in the non–cardiac-death group (2.44±0.57 versus 1.91±0.59, $P<0.0001$; Table 2).

Univariate and Multivariate Predictors of Cardiac Death

Table 3 shows the results of univariate and multivariate Cox proportional hazards model analyses for cardiac death. In the univariate analysis, log BNP, left ventricular ejection fraction, history of heart failure, heart rate, and male gender were predictive factors. In the multivariate analysis, log BNP was the only independent predictor of cardiac death.

TABLE 3. Univariate and Multivariate Relations for Prediction of Cardiac Death

	Univariate		Multivariate	
	χ^2	P	χ^2	P
Log BNP	20.06	<0.0001	7.003	0.008
LVEF (%)	7.354	0.007	...	...
History of heart failure	7.304	0.007	...	...
Heart rate, bpm	4.228	0.040	...	...
Male gender	4.096	0.043	...	...
Anterior MI	...	...	...	...
ACEI or β-blocker	...	...	...	...
History of renal dysfunction	...	...	...	...
Age, y	...	...	...	...
History of LVH	...	...	...	...
Revascularization	...	...	...	...

LVEF indicates left ventricular ejection fraction; anterior MI, patients with anterior myocardial infarction; and LVH, left ventricular hypertrophy.

*Including percutaneous coronary intervention, thrombolytic therapy, and CABG.

Kaplan-Meier Survival Analysis

We examined the sensitivity and specificity of various cutoff values of log BNP for predicting survival and created receiver operating characteristic curves. The best value of log BNP with the highest sensitivity and specificity was 2.26, equivalent to a BNP level of up to 180 pg/mL (Figure 1). Figure 2 shows that the survival rates were significantly higher in patients with log BNP <2.26 than in patients with log BNP ≥2.26.

Discussion

During the follow-up period, 23 patients died of cardiac death. The plasma BNP level 3 to 4 weeks after the onset of AMI was significantly higher in the cardiac death group (n=23) than in the non–cardiac-death group (n=122). We examined the sensitivity and specificity of various cutoff values of log BNP for predicting survival. We created

TABLE 2. Hemodynamic Parameters and BNP Levels

	Non–Cardiac-Death (n=122)	Cardiac Death (n=23)	P
Log BNP	1.91±0.59 (81±4 pg/mL)	2.44±0.57 (277±4 pg/mL)	<0.0001
Hemodynamics			
Heart rate, bpm	71±13	80±25	NS
Mean blood pressure, mm Hg	97±15	95±23	NS
SVR, dyne·s·cm^{-5}	1786±52	2209±1039	NS
PVR, dyne·s·cm^{-5}	141±76	223±127	0.0280
LVEDP, mm Hg	11±6	18±5	0.0002
LVEF, %	56±17	44±16	0.0064
CI, L·min^{-1}·m^{-2}	2.3±0.5	2.8±0.6	0.0040

Values are mean±SD. SVR indicates systemic vascular resistance; PVR, pulmonary vascular resistance; LVEDP, left ventricular end-diastolic pressure; LVEF, left ventricular ejection fraction; and CI, cardiac index.

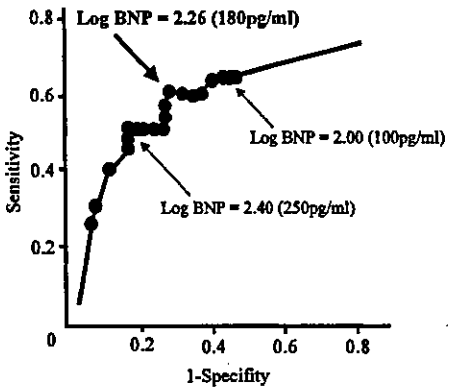

Figure 1. Receiver operating characteristic curves of BNP level for predicting cardiac death. True-positive rates (sensitivity) and false-positive rates (1-specificity) are plotted for various log BNP cutoff values for predicting cardiac death.

receiver operating characteristic curves and concluded that the best cutoff value of log BNP was 2.26, equivalent to a plasma BNP level of 180 pg/mL. The Cox proportional hazards model analysis showed that plasma BNP level was an independent predictor of cardiac death. The survival rate was significantly higher in the patients with log BNP <2.26 (equivalent to a plasma BNP level of up to 180 pg/mL) than in those with log BNP ≥2.26. This plasma BNP level for predicting cardiac events is almost the same as in previous reports.[29–32]

The present study began just after the discovery of BNP, and an antibody for BNP was created by our research group.[9,23] Thus, we were able to follow up patients for a mean period of 58.6 months for all patients, with mean follow-up periods of 41.3 months for the cardiac death group and 61.9 months for the non–cardiac-death group. We demonstrated that the plasma BNP level measured at 3 to 4 weeks after AMI onset was a significant prognostic marker of AMI in this long-term follow-up study.

There have been several reports indicating that the plasma BNP level obtained in the acute phase of AMI can be used as a prognostic marker for patients with AMI[31–37]; however, there are no reports on sampling at 3 to 4 weeks after the onset of AMI. In the present study, we performed BNP sampling at 3 to 4 weeks after AMI onset. Because the changing pattern of the plasma BNP level in patients with AMI is dynamic,[13] the timing

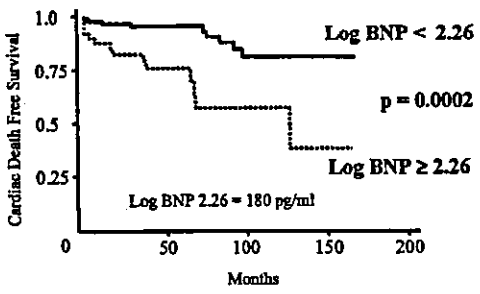

Figure 2. Kaplan-Meier survival curves of cumulative survival rates in patients with AMI divided into 2 groups according to log BNP values. Patients with log BNP ≥2.26 differed significantly from patients with log BNP values below this cutoff point.

of the blood sampling is an important matter. The first peak of plasma BNP was shown ~20 hours after AMI onset, and the second peak was shown at approximately the fifth day after onset. Plasma BNP levels in the second peak would reflect the degree of ventricular remodeling after AMI.[13] We considered that timing the blood sampling to occur just at the second peak might be ideal to predict prognosis; however, it is quite difficult to obtain the blood sample just at the second peak, because the authentic second peak of plasma BNP varies among patients with AMI. Given this background, a sampling point of 3 to 4 weeks after AMI onset appears better, because plasma BNP levels would be quite stable during this phase, as shown in our previous report.[13] The results of the present study revealed that a sampling time at 3 to 4 weeks after the onset of AMI in addition to the acute phase would provide prognostic insights, as previously speculated.[31,38]

In the present study, the number of patients taking ACE inhibitors (ACEIs) and/or β-blockers appears to be relatively low compared with recent studies[39–43]; it seems that historical background plays a role in accounting for this. There were many patients who participated in the present study around 1995; the rate of calcium channel blocker prescriptions was very high in Japan during that time. We prescribed calcium channel blockers for many patients with AMI, in part because we expected calcium channel blockers to prevent coronary artery spasm, which commonly occurs in Japanese patients.[44] Of course, the use of ACEIs or β-blockers in addition to calcium channel blockers is increasing even now in Japan. It has been reported that ACEIs are useful in the treatment of heart failure after AMI[39–42]; thus, it would be highly recommended that an ACEI be prescribed, or that the dose of the ACEI be increased, if the plasma BNP level is elevated 3 to 4 weeks after the onset of AMI. In addition, an aldosterone antagonist would be useful in the treatment of AMI.[45] In the present study, baseline medications, such as ACEIs or β-blockers, were not related to plasma BNP levels (data not shown) or the prognosis of the study patients (Table 3).

In our previous report, we stated that the biphasic pattern of the plasma BNP level indicated poor ventricular function after AMI, whereas the monophasic pattern did not.[13] Plasma BNP levels at 3 to 4 weeks after AMI onset were higher in the biphasic pattern than in the monophasic pattern. This observation and the present data suggest that the biphasic pattern would indicate a poor prognosis after AMI.

In the present long-term follow-up study, we found that plasma levels of BNP measured at 3 to 4 weeks after AMI were a prognostic marker statistically; however, the sample size was limited. Thus, it might be necessary to perform analysis on a larger scale in another series of studies. It is also necessary to examine how BNP levels at 3 to 4 weeks after the onset of AMI affect the subsequent treatment, including medical therapies and implantation of an internal defibrillator.

In conclusion, the plasma BNP level measured 3 to 4 weeks after the onset of AMI is a significant prognostic marker of AMI, as determined by this long-term follow-up study.

Acknowledgments

This study was supported in part by grants-in-aid for the Ministry of Education, Culture, Sports, Science, and Technology, Tokyo [B

(2)-15390248 and B (2)-15390249], the Ministry of Health, Labor and Welfare, Tokyo (14C-4 and 14A-1), and the Smoking Research Foundation, Tokyo.

References

1. Laragh JH. Atrial natriuretic hormone, the renin-aldosterone axis, and blood pressure–electrolyte homeostasis. *N Engl J Med.* 1985;313: 1330–1340.
2. Needleman P, Greenwald JE. Atriopeptin: a cardiac hormone intimately involved in fluid, electrolyte and blood-pressure homeostasis. *N Engl J Med.* 1986;314:828–834.
3. Floras JS. Sympathoinhibitory effects of atrial natriuretic factor in normal humans. *Circulation.* 1990;81:1860–1873.
4. Burnett JC Jr, Kao PC, Hu DC, et al. Atrial natriuretic peptide elevation in congestive heart failure in the human. *Science.* 1986;231:1145–1147.
5. Raine AEG, Erne P, Burgisser E, et al. Atrial natriuretic peptide and atrial pressure in patients with congestive heart failure. *N Engl J Med.* 1986; 315:533–537.
6. Saito Y, Nakao K, Nishimura K, et al. Clinical application of atrial natriuretic polypeptide in patients with congestive heart failure: beneficial effects on left ventricular function. *Circulation.* 1987;76:115–124.
7. Yoshimura M, Yasue H, Morita E, et al. Hemodynamic, renal, and hormonal responses to brain natriuretic peptide infusion in patients with congestive heart failure. *Circulation.* 1991;84:1581–1588.
8. Yasue H, Obata K, Okumura K, et al. Increased secretion of atrial natriuretic polypeptide (ANP) from the left ventricle in the patients with dilated cardiomyopathy. *J Clin Invest.* 1989;83:46–51.
9. Mukoyama M, Nakao K, Hosoda K, et al. Brain natriuretic peptide as a novel cardiac hormone in humans: evidence for an exquisite dual natriuretic peptide system, atrial natriuretic peptide and brain natriuretic peptide. *J Clin Invest.* 1991;91:1402–1412.
10. Yasue H, Yoshimura M, Sumida H, et al. Localization and mechanism of secretion of B-type natriuretic peptide in comparison with those of A-type natriuretic peptide in normal subjects and patients with heart failure. *Circulation.* 1994;90:195–203.
11. Yoshimura M, Yasue H, Okumura K, et al. Different secretion patterns of atrial natriuretic peptide and brain natriuretic peptide in patients with congestive heart failure. *Circulation.* 1993;87:464–469.
12. Nakagawa O, Ogawa Y, Itoh H, et al. Rapid transcriptional activation and early MRNA turnover of brain natriuretic peptide in cardiocyte hypertrophy. *J Clin Invest.* 1995;96:1280–1287.
13. Morita E, Yasue H, Yoshimura M, et al. Increased plasma levels of brain natriuretic peptide in patients with acute myocardial infarction. *Circulation.* 1993;88:82–91.
14. de Lemos JA, Morrow DA, Bentley JH, et al. The prognostic value of B-type natriuretic peptide in patients with acute coronary syndromes. *N Engl J Med.* 2001;345:1014–1021.
15. Sumida H, Yasue H, Yoshimura M, et al. Comparison of secretion pattern between A-type and B-type natriuretic peptides in patients with old myocardial infarction. *J Am Coll Cardiol.* 1995;25:1105–1110.
16. Mukoyama M, Nakao K, Obata K, et al. Augmented secretion of brain natriuretic peptide in acute myocardial infarction. *Biochem Biophys Res Commun.* 1991;180:431–436.
17. Kojima M, Minamoto N, Kangawa K, et al. Cloning and sequence analysis of cDNA encoding a precursor for rat brain natriuretic peptide. *Biochem Biophys Res Commun.* 1989;159:1420–1426.
18. Kushner I. The phenomenon of the acute phase response. *Ann N Y Acad Sci.* 1982;389:39–48.
19. Harada E, Nakagawa O, Yoshimura M, et al. Effect of interleukin-1 beta on cardiac hypertrophy and production of natriuretic peptides in rat cardiocyte culture. *J Mol Cell Cardiol.* 1999;31:1997–2006.
20. Shubeita HE, McDonough PM, Harris AN, et al. Endothelin induction of inositol phospholipid hydrolysis, sarcomere assembly, and cardiac gene expression in ventricular myocytes: a paracrine mechanism for myocardial cell hypertrophy. *J Biol Chem.* 1990;265:20555–20562.
21. Baker KM, Aceto JF. Angiotensin II stimulation of protein synthesis and cell growth in chick heart cells. *Am J Physiol Heart Circ Physiol.* 1990;259:610–618.
22. Conti E, Andreotti F, Sciahbasi A, et al. Markedly reduced insulin-like growth factor-1 in the acute phase of myocardial infarction. *J Am Coll Cardiol.* 2001;38:26–32.
23. Saito Y, Nakao K, Itoh H, et al. Brain natriuretic peptide is a novel cardiac hormone. *Biochem Biophys Res Commun.* 1989;158:360–368.
24. Sudoh T, Kangawa K, Minamino N, et al. A new natriuretic peptide in porcine brain. *Nature.* 1988;332:78–81.
25. Mukoyama M, Nakao K, Saito Y, et al. Human brain natriuretic peptide, a novel cardiac hormone. *Lancet.* 1990;335:801–802.
26. Mukoyama M, Nakao K, Saito Y, et al. Increased human brain natriuretic peptide in congestive heart failure. *N Engl J Med.* 1990;323:757–758.
27. Kono M, Yamaguchi A, Tsuji T, et al. An immunoradiometric assay for brain natriuretic peptide in human plasma. *Kaku Igaku.* 1993;13:2–7.
28. Yasue H, Yoshimura M, Jougasaki M, et al. Plasma levels of brain natriuretic peptide in normal subjects and patients with chronic congestive heart failure: measurement by immunoradiometric assay (IRMA). *Horm Clin.* 1993;41:397–403.
29. Anand IS, Fisher LD, Chiang YT, et al, for the Val-HeFT Investigators. Changes in brain natriuretic peptide and norepinephrine over time and mortality and morbidity in the Valsartan Heart Failure Trial (Val-HeFT). *Circulation.* 2003;107:1278–1283.
30. Berger R, Huelsman M, Strecker K, et al. B-type natriuretic peptide predicts sudden death in patients with chronic heart failure. *Circulation.* 2002;105:2392–2397.
31. Omland T, Aakvaag A, Bonarjee VV, et al. Plasma brain natriuretic peptide as an indicator of left ventricular systolic function and long-term survival after acute myocardial infarction: comparison with plasma atrial natriuretic peptide and N-terminal proatrial natriuretic peptide. *Circulation.* 1996;93:1963–1969.
32. Richards AM, Nicholls MG, Espiner EA, et al. B-type natriuretic peptides and ejection fraction for prognosis after myocardial infarction. *Circulation.* 2003;107:2786–2792.
33. Arakawa N, Nakamura M, Aoki H, et al. Plasma brain natriuretic peptide concentrations predict survival after acute myocardial infarction. *J Am Coll Cardiol.* 1996;27:1656–1661.
34. Darbar D, Davidson NC, Gillespie N, et al. Diagnostic value of B-type natriuretic peptide concentrations in patients with acute myocardial infarction. *Am J Cardiol.* 1996;78:284–287.
35. Palmer BR, Pilbrow AP, Yandle TG, et al. Angiotensin-converting enzyme gene polymorphism interacts with left ventricular ejection fraction and brain natriuretic peptide levels to predict mortality after myocardial infarction. *J Am Coll Cardiol.* 2003;41:729–736.
36. James SK, Lindahl B, Siegbahn A, et al. N-terminal pro-brain natriuretic peptide and other risk markers for the separate prediction of mortality and subsequent myocardial infarction in patients with unstable coronary artery disease. *Circulation.* 2003;108:275–281.
37. Omland T, Persson A, Ng L, et al. N-terminal pro-B-type natriuretic peptide and long-term mortality in acute coronary syndromes. *Circulation.* 2002;106:2913–2918.
38. Bonow RO. New insights into the cardiac natriuretic peptides. *Circulation.* 1996;93:1946–1950.
39. Pfeffer MA, Braunwald E, Moye LA, et al. Effect of captopril on mortality and morbidity in patients with left ventricular dysfunction after myocardial infarction: results of the Survival And Ventricular Enlargement trial: the SAVE Investigators. *N Engl J Med.* 1992;327: 669–677.
40. Køber L, Torp-Pedersen C, Carlsen JE, et al. A clinical trial of the angiotensin-converting-enzyme inhibitor trandolapril in patients with left ventricular dysfunction after myocardial infarction: Trandolapril Cardiac Evaluation (TRACE) Study Group. *N Engl J Med.* 1995;333:1670–1676.
41. Hall AS, Murray GD, Ball SG. Follow-up study of patients randomly allocated ramipril or placebo for heart failure after acute myocardial infarction: AIRE Extension (AIREX) Study: Acute Infarction Ramipril Efficacy. *Lancet.* 1997;349:1493–1497.
42. Yusuf S, Sleight P, Pogue J, et al. Effects of an angiotensin-converting–enzyme inhibitor, ramipril, on cardiovascular events in high-risk patients: the Heart Outcomes Prevention Evaluation Study Investigators. *N Engl J Med.* 2000;342:145–153.
43. ISIS-1 (First International Study of Infarct Survival) Collaborative Group. Randomised trial of intravenous atenolol among 16027 cases of suspected acute myocardial infarction: ISIS-1. *Lancet.* 1986;2:57–66.
44. Yasue H, Kugiyama K. Coronary spasm: clinical features and pathogenesis. *J Intern Med.* 1997;36:760–765.
45. Pitt B, Remme W, Zannad F, et al. Eplerenone, a selective aldosterone blocker, in patients with left ventricular dysfunction after myocardial infarction. *N Engl J Med.* 2003;348:1309–1321.

Serum leptin level is a regulator of bone mass

F. Elefteriou*†‡, S. Takeda*†‡§, K. Ebihara¶, J. Magre‖, N. Patano*, C. Ae Kim**, Y. Ogawa§††, X. Liu*, S. M. Ware*, W. J. Craigen*, J. J. Robert‡‡, C. Vinson§§, K. Nakao¶, J. Capeau‖, and G. Karsenty*†¶¶

*Department of Molecular and Human Genetics, †Bone Disease Program of Texas, Baylor College of Medicine, Houston, TX 77030; ¶Department of Medicine and Clinical Science, Kyoto University Graduate School of Medicine, Kyoto 606-8507, Japan; ‖Institut National de la Santé et de la Recherche Médicale U.402, Faculté de Médecine St-Antoine, 75012 Paris, France; **Genetica Instituto da Criança, CEP 05403-900, São Paulo, Brazil; §Center of Excellence Program for Frontier Research on Molecular Destruction and Reconstruction of Tooth and Bone, Tokyo Medical and Dental University, Tokyo 101-0062, Japan; ††Department of Molecular Medicine and Metabolism, Medical Research Institute, ‡‡Department of Pediatric Diabetology, Necker Hospital, 75730 Paris, France; and §§Laboratory of Biochemistry, National Cancer Institute, Bethesda, MD 20892

Communicated by Pierre Chambon, Institut de Génétique et de Biologie Moléculaire et Cellulaire, Strasbourg, France, January 5, 2004 (received for review October 29, 2003)

Leptin is a powerful inhibitor of bone formation *in vivo*. This antiosteogenic function involves leptin binding to its receptors on ventromedial hypothalamic neurons, the autonomous nervous system and β-adrenergic receptors on osteoblasts. However, the mechanisms whereby leptin controls the function of ventromedial hypothalamic antiosteogenic neurons remain unclear. In this study, we compared the ability of leptin to regulate body weight and bone mass and show that leptin antiosteogenic and anorexigenic functions are affected by similar amounts of leptin. Using a knock-in of *LacZ* in the *leptin* locus, we failed to detect any leptin synthesis in the central nervous system. However, increasing serum leptin level, even dramatically, reduced bone mass. Conversely, reducing serum-free leptin level by overexpressing a soluble receptor for leptin increased bone mass. Congruent with these results, the high bone mass of lipodystrophic mice could be corrected by restoring serum leptin level, suggesting that leptin is an adipocyte product both necessary and sufficient to control bone mass. Consistent with the high bone mass phenotype of lipodystrophic mice, we observed an advanced bone age, an indirect reflection of premature bone formation, in lipodystrophic patients. Taken together, these results indicate that adipocyte-derived circulating leptin is a determinant of bone formation and suggests that leptin antiosteogenic function is conserved in vertebrates.

A growing body of work has established the central role of the hypothalamus in the regulation of bone formation by osteoblasts (1–4). The thrust of this influence is exerted by neurons located in the ventromedial hypothalamus. These neurons are themselves the target of leptin, which was demonstrated to be a powerful antiosteogenic hormone (1). Based on chemical lesioning, genetic manipulations, and pharmacological experiments, hypothalamic neurons mediating leptin antiosteogenic and anorexigenic functions could be distinguished. Moreover, genetic evidence indicates that, peripherally, the sympathetic nervous system mediates preferentially leptin antiosteogenic function (2). Thus leptin uses distinct pathways to regulate bone mass and body weight.

The discovery of leptin antiosteogenic function was a surprise for at least two reasons. First, it was not the function for which leptin was molecularly cloned, and this implied a more pleiotropic role for this hormone than originally anticipated. Second, and more important physiologically, the high bone mass of leptin signaling-deficient mice existed despite the presence of an increase in bone resorption caused by the hypogonadism of these mice. This coexistence of hypogonadism and high bone mass is pivotal to appreciate the physiological importance of leptin antiosteogenic function. Indeed, it established genetically that leptin signaling plays a dominant role over gonadal function in the regulation of bone mass and thereby implied that this is a major function of leptin.

In the present study we addressed several questions raised by the identification of leptin as an antiosteogenic hormone. Specifically, can we assess *in vivo* the relative importance of leptin antiosteogenic and anorexigenic functions, can we determine whether the blood circulation is the main, if not the only, mean whereby leptin regulates bone mass, and, lastly, can we provide evidence suggesting a conservation of this function during evolution?

Materials and Methods

Animals. *Ob/+* mice were obtained from The Jackson Laboratory. Generation of *A-ZIP/F-1* and *SAP-Leptin* transgenic mice has been reported (5–7). *ApoE-leptin* transgenic mice were generated by cloning the mouse *Leptin* cDNA 3′ of the liver specific Apolipoprotein E promoter and 5′ of the liver-specific enhancer sequence contained in the pLiv7 construct. *ApoE-ObRe* mice were generated by inserting the *ObRe* cDNA of the *ObR* gene into pLiv7. *ApoE-leptin* and *ApoE-ObRe* mice were generated on a FVB and C57BL6J background, respectively, and two independent strains were analyzed for each strain. The knock-in of nuclear *LacZ* gene into the *Leptin* locus was generated by replacing exon 3 of the *leptin* coding sequence by the nuclear *lacZ* gene fused to the *neomycin*-resistant gene. Electroporation of embryonic stem (ES) cells, subsequent selection, injection of positive clones into blastocysts, and implantation into pseudopregnant females were done according to standard protocols (8).

Intracerebroventricular (ICV) Infusions. A 28-gauge cannula (Brain infusion kit II, Alza) infusing human leptin (Sigma) for 28 days was implanted into the third ventricle of 2-month-old C57BL6J female mice, as described (1). The cannula was connected to an osmotic pump (Alza) placed in the dorsal s.c. space of the animal.

5-Bromo-4-chloro-3-indolyl β-D-Galactoside (X-Gal) Staining. Animals were killed at 2 months of age, and the tissues were dissected in cold PBS. X-Gal staining was done according to standard protocols (9). Specimens were postfixed in phosphate buffered formalin for 5 h, dehydrated, cleared, and embedded in paraffin. Specimens were cut at 7 μm, and nuclei were stained with Hoechst reagent.

Leptin-Induced STAT3-luc Reporter Analysis. Recombinant histidine-tagged rObRe was produced *in vitro* in 293EBNA cells and purified on a nickel-nitrilotriacetic affinity column (Qiagen, Valencia, CA) according to the manufacturer's recommendations (a detailed procedure is available in *Supporting Text*, which is published as supporting information on the PNAS web site). HEK293 cells stably expressing *ObRb* were transfected by Fugene reagent (Roche Diagnostics) with a STAT3-Luc leptin-

Abbreviations: ICV, Intracerebroventricular; X-Gal, 5-bromo-4-chloro-3-indolyl β-D-galactoside.

†F.E. and S.T. contributed equally to this work.

¶¶To whom correspondence should be addressed. E-mail: karsenty@bcm.tmc.edu.

www.pnas.org/cgi/doi/10.1073/pnas.0308744101

responsive construct (kindly provided by C. Li, University of Texas Southwestern, Dallas) and a β-galactosidase reporter construct for normalization. Recombinant human leptin (0.5 nM, Sigma) and rObRe (5 and 50 nM) were preincubated for 30 min at room temperature before addition to the cells for 3 h. Luciferase and β-galactosidase activities were measured according to standard protocols (8).

Gel Chromatography. ^{125}I-leptin was used to trace bound and free leptin from serum after fractionation by FPLC (Amersham Pharmacia FPLC system) on a High load Superdex 200–16/60 column (Amersham Pharmacia) calibrated by using Bio-Rad gel filtration standards. A detailed procedure is available in *Supporting Text*.

Histology. Histological analyses were performed on undecalcified specimen as described (1). Static and dynamic histomorphometric analyses were performed according to standard protocols (10) using the Osteomeasure Analysis System (Osteometrics, Atlanta). Four to 10 animals were analyzed for each group. Controls for each group were WT littermates of the same sex, age, and genetic background. Statistical significance was assessed by Student's *t* test. Results are expressed as mean ± SE.

Serum Chemistry. Total leptin serum levels were measured by using an immunoassay kit from Linco Diagnostics, following the manufacturer's instructions.

Osseous Age Measurements. Osseous age was rated by a single radiologist unaware of the patient's chronological ages on radiographs of left hands and wrists, using the method of Greulich and Pyle (11).

Results

Comparison of Antiosteogenic and Anorexigenic Functions of Leptin. The existence of a high bone mass phenotype in the face of an increase in bone resorption in leptin signaling-deficient mice suggests that leptin antiosteogenic activity is a major function of this hormone. To test this contention *in vivo* we used ICV infusion of leptin in WT mice as a bioassay. We infused different amounts of this hormone for 1 month and used body weight and bone volume as indicators of leptin bioactivity (Fig. 1*A*). As reported (12), ICV infusion of leptin at 8 and, to a lesser extent, 4 ng/h significantly decreased body weight, whereas lower leptin doses failed to affect it significantly (Fig. 1*B*). ICV infusion of leptin at 8, 4, and even 2 ng/h significantly reduced bone mass of WT mice (Fig. 1*C*). The fact that similar amounts of leptin were needed to affect body weight and bone mass suggests that leptin anorexigenic and antiosteogenic functions are of equal importance *in vivo*. This is consistent with the fact that the antiosteogenic function of leptin was uncovered in a situation strongly favoring bone loss, not bone gain.

Absence of Leptin Production in the Brain. Different observations raised the formal hypothesis that serum leptin may not regulate bone mass. For instance, it has been difficult to date to correlate bone density, an indirect assessment of bone mass, and serum leptin level in humans (13–15). Moreover, leptin antiosteogenic action was more easily achieved by ICV infusion than by peripheral injection, and lastly, leptin expression has been detected by RT-PCR and immunocytochemistry in the mouse hypothalamus (16), where leptin antiosteogenic neurons reside (2). Together, these observations suggested the possibility that leptin was produced locally in the brain and that this local production was important in understanding leptin antiosteogenic function.

To test this hypothesis we first assessed leptin expression in various parts of the brain and in fat tissue by *in situ* hybridization

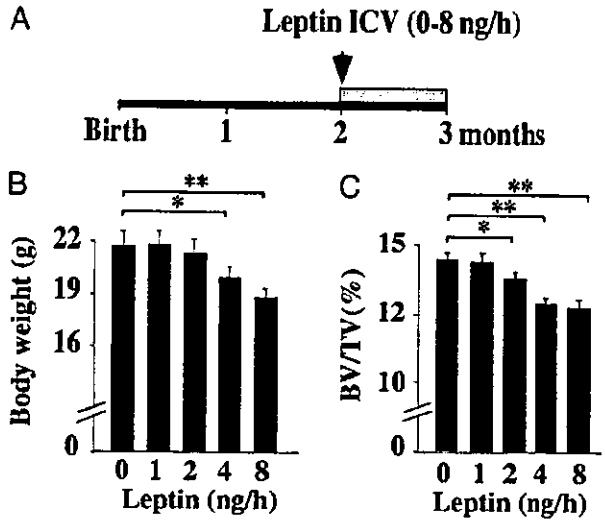

Fig. 1. Comparison of leptin antiosteogenic and anorexigenic functions. (*A*) Two-month-old C57BL6J females were infused ICV for 28 days with the indicated amount of leptin. (*B*) The lowest leptin amount that significantly decreased body weight was 4 ng/h. (*C*) The lowest leptin amount that significantly decreased bone volume over tissue volume (BV/TV, %) was 2 ng/h (n = 8; *, $P < 0.05$; **, $P < 0.005$).

(ISH). Despite several attempts, we failed to detect expression of *Leptin* in any brain area investigated at different developmental stages or postnatally, whereas fat tissues constitutively gave a strong signal (G. Eichele, personal communication). To rule out the possibility that a low level of *Leptin* transcripts, undetectable by ISH, was present in the brain as reported for other genes (9), we knocked-in the *LacZ* gene in the *Leptin* locus through homologous recombination in ES cells (Fig. 2*A*). $Lep^{LacZ/LacZ}$ mice were obese and had a high bone mass phenotype (data not shown). $Lep^{LacZ/LacZ}$ and WT littermates were analyzed for the presence of β-galactosidase activity in brain and adipose tissues. Strong X-Gal staining was observed in adipose tissue of homozygote animals (Fig. 2 *C* and *E*), whereas no staining could be detected in any brain area analyzed macroscopically and histologically (Fig. 2 *D* and *F*). Taken together, these results indicate that leptin is not produced locally in the brain, and thereby imply that circulating leptin must account for its antiosteogenic function.

Raising Serum Leptin Level Decreases Bone Mass. If circulating leptin affects bone mass, then transgenic mouse models with high serum leptin level should have a low bone mass. To determine whether this is the case, we studied two transgenic mouse strains with different serum leptin levels.

The first strain of mice was generated by using the liver-specific human serum amyloid P component (*SAP*) promoter to drive *Leptin* cDNA expression in liver (6). As reported, *SAP-leptin* transgenic mice had a moderate, i.e., 4-fold, increase in their serum leptin level compared to WT littermates (Fig. 3*A*). This resulted in a lower body weight and a complete absence of fat pads (6). Histological examination revealed that *SAP-leptin* transgenic mice also displayed a significant decrease in bone mass when compared to WT littermates, thus suggesting that serum leptin controls bone mass (Fig. 3*A*). The second leptin overexpressing mouse model was generated by using the Apolipoprotein E (*ApoE*) promoter and liver-specific enhancer (Fig. 3*B*). Northern blot analysis verified that the transgene was strongly expressed in liver (Fig. 3*B*). Accordingly, serum leptin level in *ApoE-leptin* transgenic mice was 200- to 300-fold higher than what was seen in WT littermates, at all time points analyzed

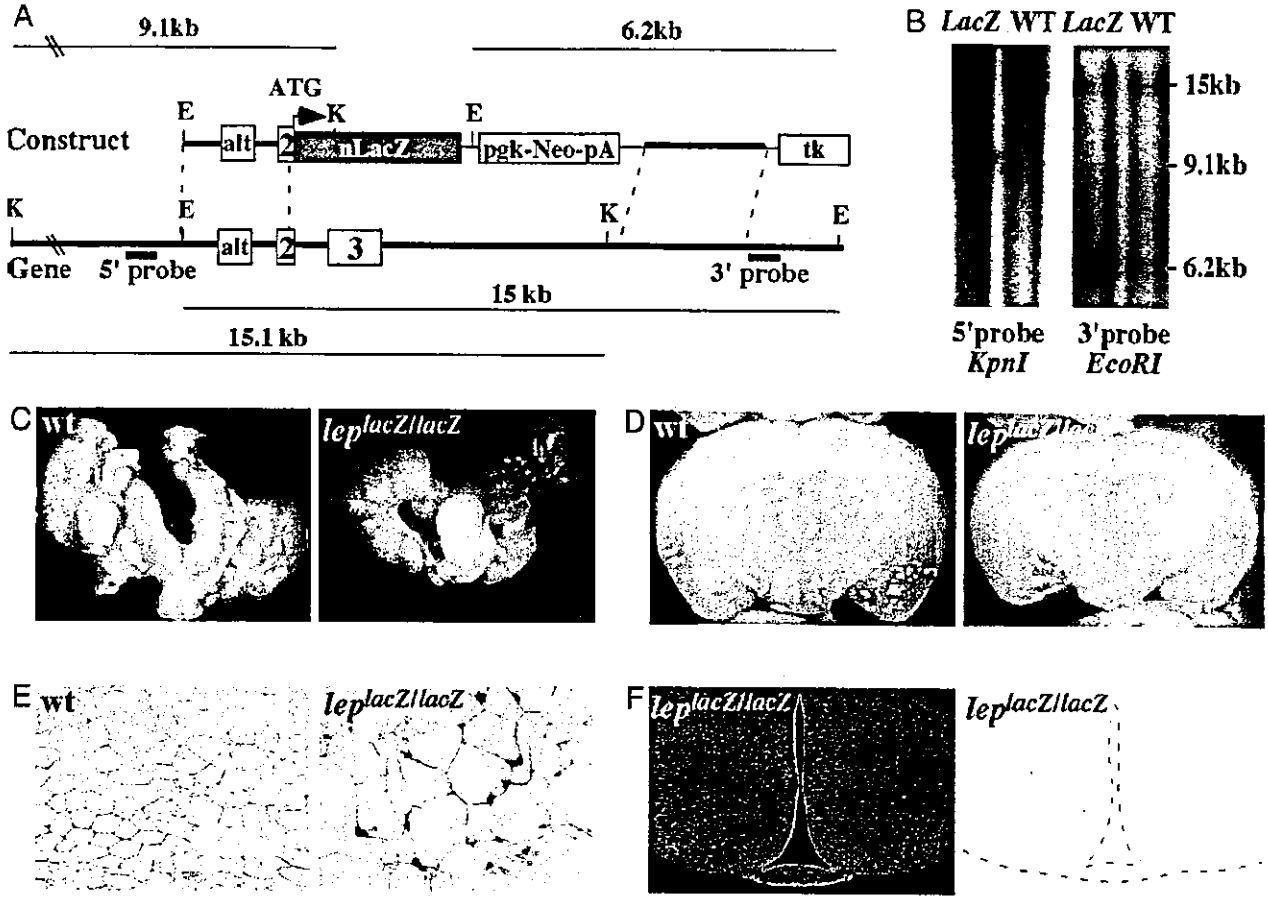

Fig. 2. Adipose tissue as the only detectable source of leptin. (*A*) Genomic organization of the *Leptin* locus and structure of the targeting vector. Probes used for Southern blots and restriction fragments are indicated. (*B*) Southern blots. The WT and *lacZ* knock-in loci gave, respectively, 15.0- and 6.2-kb bands with the 3′ probe, and 15.1- and 9.1 kb bands with the 5′ probe. E, *EcoRI*; K, *KpnI*. (*C* and *D*) X-Gal-stained gonadal adipose tissue and brain. Staining was detected exclusively in adipose tissue in $Lep^{lacZ/lacZ}$ mice. No staining was detected in brain. (*E* and *F*) Histological examination of adipose and brain tissues after X-Gal staining. Nuclear staining was readily detectable in adipocyte nuclei, but no staining was observed in any brain section. A representative brain section containing arcuate and ventromedial hypothalamus neurons counterstained with Hoescht (*Left*) and stained with X-Gal (*Right*) are shown.

(Fig. 3 *C* and *D*). This marked elevation of serum leptin level in *ApoE-leptin* transgenic mice resulted in a complete disappearance of fat pads (Fig. 3*B*) and in a decrease in food intake (data not shown), demonstrating that leptin signaling was increased in these animals. Likewise, we observed a significant decrease in bone mass in 3- and 6-month-old *ApoE-leptin* mice, regardless of the sex of the animals (Fig. 3 *C* and *D*). The low bone mass phenotype observed in *ApoE-leptin* mice was accompanied by a reduction in the bone formation rate (Fig. 3*D*). Taken together, these results demonstrate that increasing serum leptin level, even to very high levels, results in a reduction of osteoblastic activity and a subsequent low bone mass.

Reducing Serum-Free Leptin Level Increases Bone Mass. To further address the role of circulating leptin and to determine whether free, i.e., unbound, serum leptin is a determinant of bone mass, we attempted to decrease the level of circulating free leptin by transgenesis. *ObR*, the leptin receptor gene, encodes five different forms of the leptin receptor through alternative splicing. One of these forms, *ObRe*, lacks the transmembrane domain found in all other isoforms, and therefore behaves as a soluble receptor for leptin (17). By analogy with other physiological regulatory loops in bone, we reasoned that *ObRe* could serve as a decoy receptor for leptin. This would be reminiscent of the role that osteoprotegerin plays as a decoy receptor for RANK-L, a critical regulator of bone resorption (18). The potency of ObRe to inhibit leptin signaling was first established *in vitro* by showing that recombinant ObRe inhibits the activity of a STAT3-dependent luciferase reporter construct, induced by leptin treatment of 293 cells expressing the ObRb receptor (Fig. 4*A*). We then used ApoE regulatory elements to overexpress *ObRe* in liver and systemically (Fig. 4*B*). *ApoE-ObRe* transgenic mice had a moderate but nonsignificant increase in body weight, fat pad weight, and bone mass (data not shown). We reasoned that this relative lack of efficacy of the *ObRe* transgene could be explained by a serum leptin level still too high relative to the level of *ObRe* expression in *ApoE-ObRe* transgenic mice. If this was the case, then transferring the *ObRe* transgene to mice with a lower leptin level should uncover any phenotypic abnormalities secondary to the decrease in circulating free leptin. Serum leptin level is lower in *Ob*/+ mice than in WT mice (4.01 ± 0.3 ng/ml in *Ob*/+ mice vs. 5.7 ± 0.1 ng/ml in WT mice, $P < 0.05$, $n = 12$ per group). We therefore crossed them with *ApoE-ObRe* mice to generate *ApoE-ObRe;Ob*/+ mice.

Protein size fractionation through gel filtration indicated that serum-free leptin level was reduced in *ApoE-ObRe;Ob*/+ compared to *Ob*/+ mice. As shown in Fig. 4*C*, free leptin (fraction 90, 16–17 kDa) was efficiently separated from the bound form of leptin (fraction 58, 310 kDa). The size of the bound form of leptin is consistent with leptin binding to dimers of ObRe (19).

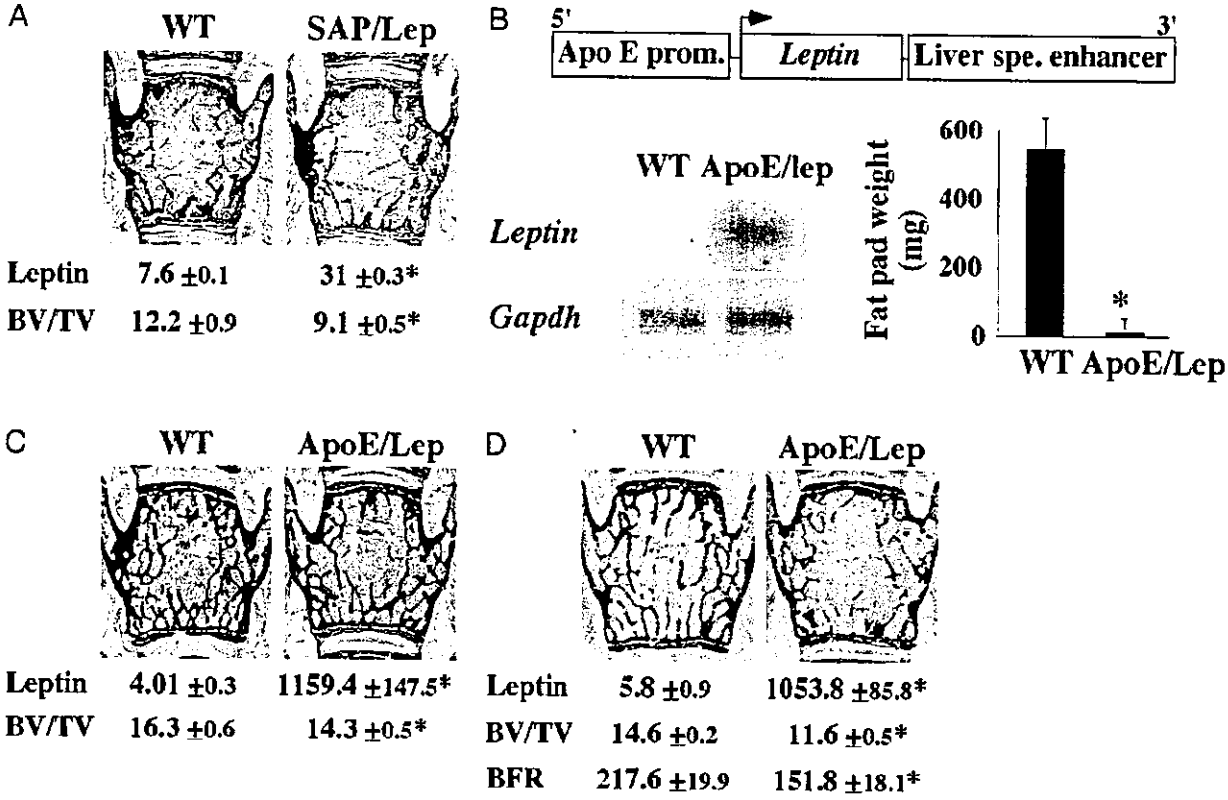

Fig. 3. Increasing serum leptin reduces bone mass. (*A*) Six-month-old *SAP-Leptin* mice are mildly hyperleptinemic (leptin, ng/ml) and display a low bone volume over tissue volume (BV/TV, %) compared to controls ($n = 4$; *, $P < 0.05$). (*B*) Schematic representation of the *ApoE/Lep* transgene. Northern blot analysis confirmed the expression of the transgene in liver. *ApoE/Lep* mice have no fat pads ($n = 8$; *, $P < 0.01$). (*C* and *D*) Compared to controls, *ApoE/lep* mice at 3 (*C*) and 6 (*D*) months of age displayed a reduced bone volume and a decreased BFR/BS ($\mu m^3/\mu m^2$ per yr) despite a 200- to 300-fold increase in serum leptin level (ng/ml) ($n = 8$; *, $P < 0.05$).

Free leptin fraction represented ~65% of total leptin in the *Ob*/+ mouse serum and only 5.4% in *ApoE-ObRe;Ob*/+ mouse serum. This decrease in circulating free leptin led to a significant increase in the fat pad weight of these mice (Fig. 4*D*) and, as hypothesized, to a significant increase in bone mass compared to *Ob*/+ mice (Fig. 4*E*). These results establish that circulating free leptin is a determinant of bone mass.

Leptin, Lipodystrophy, and Bone Mass. We have previously shown that *A-ZIP/F1* lipodystrophic mice have a high bone mass phenotype, indicating that adipocytes are necessary for the control of bone mass (1). To test whether leptin is the adipocyte-derived gene product responsible of this phenotype, we crossed the *A-ZIP/F1* mice with the *SAP-Leptin* overexpressing mice and compared the bone volume of the double transgenic mice to the one of *A-ZIP/F1* and WT mice. In contrast to *A-ZIP/F1* mice, *A-ZIP/F1;SAP-Leptin* mice had a normal bone mass (Fig. 5), indicating that leptin is an adipocyte gene product that is both necessary and sufficient to control bone formation.

The critical role of leptin in the control of bone mass in mice raised the question of its role in humans. The high bone mass phenotype observed in lipodystrophic mice suggested that, if leptin antiosteogenic function was conserved, lipodystrophic patients should have evidence of an increased bone formation. This is obviously a difficult question to address for several reasons. First, ethical considerations prevent the collection of bone biopsies from these patients. Second, there are no weight- and age-matched controls that can be used in indirect methods to measure bone density. Because of these limitations, we used as an indirect but suggestive indicator of bone formation the osseous age of prepubertal patients affected by congenital generalized lipodystrophy. All lipodystrophic patients displayed low to undetectable circulating levels of leptin (Table 1) and had, regardless of their sex, a marked advance in bone age. The same advance in bone age was also observed in a single leptin-deficient child to whom we had access to (J. Licino, personal communication). These correlative data are in agreement with what was observed in lipodystrophic mice, and suggest that serum leptin in humans also controls bone homeostasis.

Discussion

Our studies show that leptin is equipotent in the control of body weight and bone mass and that circulating leptin, at low or high concentrations, regulates bone mass. Furthermore, available evidence suggests that this function of leptin is, like its other functions, conserved between mouse and human.

The fact that leptin antiosteogenic function was uncovered in animals that have an increased bone resorption was already a suggestive indication that it should be a major function of this hormone. That leptin antiosteogenic function could be achieved with a dose similar to the one needed to affect body weight in WT mice confirms experimentally this contention. This observation, and others previously reported, suggest that leptin is a general neuroendocrine regulator of body weight, reproduction and bone mass (1). A parallel exists between the pleiotropic functions of leptin and for example the multiple functions of insulin. Indeed, besides its crucial role in the regulation of blood glucose level that led to its identification, it is now evident that insulin has other important functions, such as regulating life span in invertebrates and vertebrates (20–22).

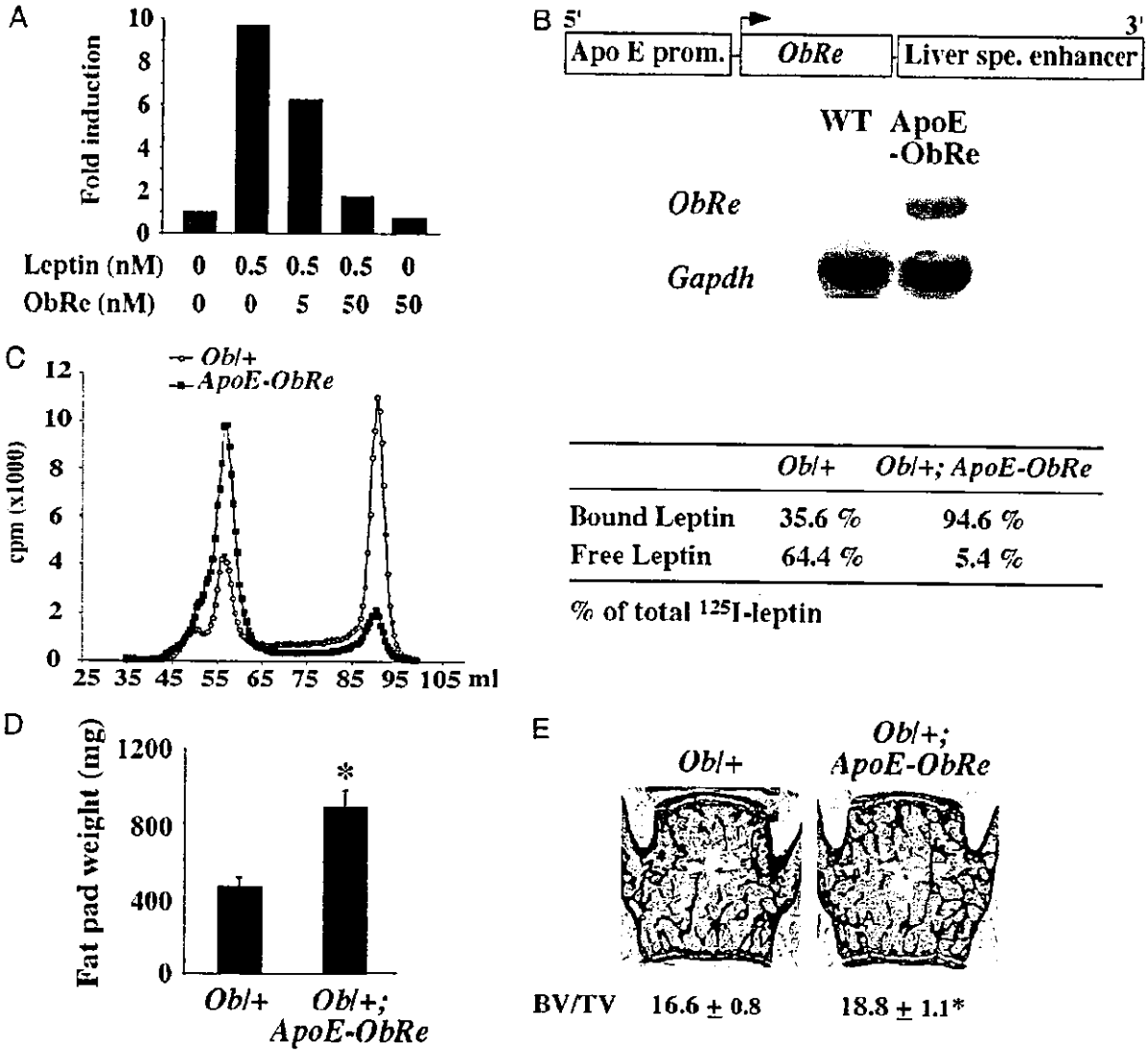

Fig. 4. Decreasing serum free leptin level increases bone mass. (*A*) Leptin-induced STAT3 reporter activity is decreased by ObRe treatment. (*B*) Schematic representation of the *ApoE-ObRe* transgene. Northern blot analysis confirmed the expression of the transgene in liver. (*C*) Size fractionation chromatogram. Marked reduction in serum free leptin level in *Ob/+; ApoE-ObRe* mice compared to *Ob/+* mice (a representative chromatogram is shown, $n = 4$). (*D* and *E*) Three-month-old *Ob/+; ApoE-ObRe* mice had a significant increase in gonadal fat pad weight (*D*) and in bone volume over tissue volume (BV/TV, %) (*E*) compared to controls ($n = 8$; *, $P < 0.05$).

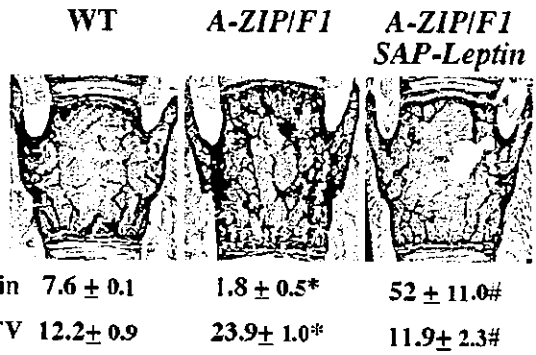

Fig. 5. Leptin and bone mass in lipodystrophic mice. Expression of the *SAP-leptin* transgene in the *A-ZIP/F1* genetic background increased serum leptin levels (ng/ml) and corrected the high bone mass of *A-ZIP/F1* mice ($n = 4$; *, controls versus *A-ZIP/F1*, $P < 0.05$; #, *A-ZIP/F1* versus *A-ZIP/F1;SAP-leptin*, $P < 0.05$).

Several lines of evidence establish that neuronal antiosteogenic pathways are controlled by serum leptin level. First, we failed to detect *Leptin* transcripts in the hypothalamus or elsewhere in the brain. Second, increasing serum leptin level decreased bone mass. This was true even with an extreme elevation of serum leptin level, indicating that hypothalamic neurons remain sensitive even when serum leptin level is increased >200-fold. However, the sensitivity of ventromedial hypothalamus neurons to leptin must be partially abrogated because *ApoE-leptin* mice did not have a lower bone mass than *SAP-leptin* mice. In that respect, it should be noted that A^y/a mice, which are resistant to leptin administration, have a decreased expression of neuropeptide Y (NPY) and Agouti-related peptide mRNA compared to leptin signaling-deficient mice, indicating that, despite the absence of effect on body weight, the leptin signal is still sensed to a certain extent by hypothalamic neurons in these mice (23, 24). Third, decreasing serum-free leptin level by overexpressing the leptin-soluble receptor ObRe led to an

Table 1. Lipodystrophic patients have low to undetectable serum leptin levels and an advanced bone age

	Patient							
	1	2	3	4	5	6	7	8
Sex	M	M	M	F	F	F	F	F
Leptin, ng/ml	0.23	ND	ND	0.68	1.4	0.22	0.37	0.25
Chronological age	6.0 w	5.0 m	1.7 y	1.9 y	3.0 y	4.0 y	8.0 y	13.0 y
Bone age	4.5 m	1.0 y	2.3 y	2.6 y	7.5 y	5.0 y	11.0 y	15.0 y

M, male; F, female; ND, not determined; w, weeks; m, months; y, years.

increase in bone mass. Finally this role played by circulating leptin is important to interpret other data present in the literature. For instance, although NPY-deficient mice have no bone phenotype (25), mice lacking the Y2 or both Y2 and Y4 receptors have a high bone mass phenotype and a marked decrease in serum leptin level (3, 4).

Interestingly, in terms of bone biology, a parallel can be made between ObRe, which modulates the function of leptin, the major hormonal regulator of bone formation, and osteoprotegerin, another decoy receptor regulating the activity of RANK-L, the major regulator of bone resorption (26). These results suggest that bone formation and bone resorption are controlled, at least in part, by the interplay of circulating factors and decoy receptors.

Several observations suggest that leptin antiosteogenic function, like its other functions, is conserved during evolution. First, lipodystrophic mice have a high bone mass phenotype and, as shown here, lipodystrophic patients have an advanced bone age, an indirect evidence of premature bone formation. Second, beta-blockers increase bone formation and bone mass in mice and, in humans, beta-blockers have recently been shown to reduce the incidence of fracture in osteoporotic patients (27). Taken together, these observations suggest that leptin antiosteogenic function has been conserved during evolution.

We thank Drs. Li, Eichele, Ducy, Fauré, Maachi, and Mégarbané for reagents, patients, expertise, and critical reading of the manuscript. This work was supported by National Institutes of Health Grant DK5883 and National Space Biomedical Research Institute Grant NCC9-58 (to G.K.), the Children's Nutrition Research Center (G.K. and F.E.), and the Arthritis Foundation (S.T.).

1. Ducy, P., Amling, M., Takeda, S., Priemel, M., Schilling, A. F., Beil, T., Shen, J., Vinson, C., Rueger, J. M. & Karsenty, G. (2000) *Cell* **100**, 197–207.
2. Takeda, S., Elefteriou, F., Levasseur, R., Liu, X., Zhao, L., Parker, K. L., Armstrong, D., Ducy, P. & Karsenty, G. (2002) *Cell* **111**, 305–317.
3. Baldock, P. A., Sainsbury, A., Couzens, M., Enriquez, R. F., Thomas, G. P., Gardiner, E. M. & Herzog, H. (2002) *J. Clin. Invest.* **109**, 915–921.
4. Sainsbury, A., Baldock, P. A., Schwarzer, C., Ueno, N., Enriquez, R. F., Couzens, M., Inui, A., Herzog, H. & Gardiner, E. M. (2003) *Mol. Cell. Biol.* **23**, 5225–5233.
5. Moitra, J., Mason, M. M., Olive, M., Krylov, D., Gavrilova, O., Marcus-Samuels, B., Feigenbaum, L., Lee, E., Aoyama, T., Eckhaus, M., *et al.* (1998) *Genes Dev.* **12**, 3168–3181.
6. Ebihara, K., Ogawa, Y., Masuzaki, H., Shintani, M., Miyanaga, F., Aizawa-Abe, M., Hayashi, T., Hosoda, K., Inoue, G., Yoshimasa, Y., *et al.* (2001) *Diabetes* **50**, 1440–1448.
7. Ogawa, Y., Masuzaki, H., Hosoda, K., Aizawa-Abe, M., Suga, J., Suda, M., Ebihara, K., Iwai, H., Matsuoka, N., Satoh, N., *et al.* (1999) *Diabetes* **48**, 1822–1829.
8. Ausubel, F. M. (1995) *Current Protocols in Molecular Biology* (Wiley Interscience, New York).
9. Wang, V. Y., Hassan, B. A., Bellen, H. J. & Zoghbi, H. Y. (2002) *Curr. Biol.* **12**, 1611–1616.
10. Parfitt, A. M., Drezner, M. K., Glorieux, F. H., Kanis, H. A., Malluche, H., Meunier, P. J., Ott, S. M. & Recker, R. R. (1987) *J. Bone Miner. Res.* **6**, 595–610.
11. Greulich, W. & Pyle, S. (1959) *Radiographic Atlas of Skeletal Development of the Hand and Wrist* (Stanford Univ. Press, Stanford, CA).
12. Halaas, J. L., Boozer, C., Blair-West, J., Fidahusein, N., Denton, D. A. & Friedman, J. M. (1997) *Proc. Natl. Acad. Sci. USA* **94**, 8878–8883.
13. Goulding, A. & Taylor, R. W. (1998) *Calcif. Tissue Int.* **63**, 456–458.
14. Odabasi, E., Ozata, M., Turan, M., Bingol, N., Yonem, A., Cakir, B., Kutlu, M. & Ozdemir, I. C. (2000) *Eur. J. Endocrinol.* **142**, 170–173.
15. Rauch, F., Blum, W. F., Klein, K., Allolio, B. & Schonau, E. (1998) *Calcif. Tissue Int.* **63**, 453–455.
16. Ur, E., Wilkinson, D. A., Morash, B. A. & Wilkinson, M. (2002) *Neuroendocrinology* **75**, 264–272.
17. Tartaglia, L. A., Dembski, M., Weng, X., Deng, N., Culpepper, J., Devos, R., Richards, G. J., Campfield, L. A., Clark, F. T., Deeds, J., *et al.* (1995) *Cell* **83**, 1263–1271.
18. Simonet, S., Lacey, D. L., Dunstan, C. R., Kelley, M., Chang, M. S., Luthy, R., Nguyen, H., Wooden, S., Bennett, T. & Boone, T. (1997) *Cell* **89**, 309–319.
19. Devos, R., Guisez, Y., Van der Heyden, J., White, D. W., Kalai, M., Fountoulakis, M. & Plaetinck, G. (1997) *J. Biol. Chem.* **272**, 18304–18310.
20. Lee, S. S., Kennedy, S., Tolonen, A. C. & Ruvkun, G. (2003) *Science* **300**, 644–647.
21. Murphy, C. T., McCarroll, S. A., Bargmann, C. I., Fraser, A., Kamath, R. S., Ahringer, J., Li, H. & Kenyon, C. (2003) *Nature* **424**, 277–283.
22. Bluher, M., Kahn, B. B. & Kahn, C. R. (2003) *Science* **299**, 572–574.
23. Ollmann, M. M., Wilson, B. D., Yang, Y. K., Kerns, J. A., Chen, Y., Gantz, I. & Barsh, G. S. (1997) *Science* **278**, 135–138.
24. Kesterson, R. A., Huszar, D., Lynch, C. A., Simerly, R. B. & Cone, R. D. (1997) *Mol. Endocrinol.* **11**, 630–637.
25. Elefteriou, F., Takeda, S., Liu, X., Armstrong, D. & Karsenty, G. (2003) *Endocrinology* **144**, 3842–3847.
26. Boyle, W. J., Simonet, W. S. & Lacey, D. L. (2003) *Nature* **423**, 337–342.
27. Pasco, J., Henry, M., Sanders, K., Kotowicz, M., Seeman, E. & Nicholson, G. (2004) *J. Bone Miner. Res.* **19**, 19–24.

and Decherd do not provide robust outcome data on the procedures they advocate. I consider an average fee of more than $5,000 for an operation lasting several hours to be expensive and profitable.[1]

The experience of a mystery shopper who consulted five established plastic surgeons with the same requests illustrates the lack of consensus among cosmetic surgeons about optimal therapy.[2] Both the recommended treatments and their costs ($2,900 to $14,150) varied greatly among the surgeons. Given the lack of good studies quantifying the benefits and risks of many of the cosmetic procedures and products that leading plastic surgeons now advocate and sell, and given the even scantier information on individual surgeons' outcomes, I hope the American Society of Plastic Surgeons will take a leading role in filling this void in the data.

Robert S. Stern, M.D.

Beth Israel Deaconess Medical Center
Boston, MA 02215
rstern@bidmc.harvard.edu

1. American Society of Plastic Surgeons. (Accessed July 15, 2004, at http://www.plasticsurgery.org/public-education/procedures/index.cfm.)
2. Besonen J. Does this woman need a facelift? Boston Magazine. February 2000.

Long-Term Leptin-Replacement Therapy for Lipoatrophic Diabetes

TO THE EDITOR: Oral et al. reported in 2002 that leptin treatment for a period of four months improved hyperglycemia and hypertriglyceridemia in nine female patients with lipodystrophy.[1] We report the efficacy of leptin-replacement therapy given for 12 months with the use of the same protocol in two Japanese patients. Patient 1 was an 11-year-old girl with acquired generalized lipodystrophy. She was normal at birth and in her growth. At nine years of age, cervical lymphangitis and panniculitis developed. After that, she had systematic fat loss, her body weight decreased from 38.5 kg to 26.0 kg, and diabetes emerged within two months. Treatment with pioglitazone (15 mg per day) for 10 months did not improve glycemic control. Just before starting leptin-replacement therapy, she had marked hyperglycemia (glycosylated hemoglobin, 10.0 percent), hypertriglyceridemia (1941 mg per deciliter), and severe fatty liver. Patient 2 was a 29-year-old man with congenital generalized lipodystrophy. A generalized deficiency of body fat was noticed from birth, with the onset of diabetes when he was 11 years old. Glyburide (glibenclamide) (2.5 mg per day) and voglibose (0.6 mg per day) were ineffective. Just before leptin-replacement therapy was initiated, his glycosylated hemoglobin level was 10.3 percent. He had neither hypertriglyceridemia nor fatty liver.

Patients 1 and 2 had extremely low values for body fat (5.2 percent and 4.7 percent, respectively, as measured by dual-energy x-ray absorptiometry)

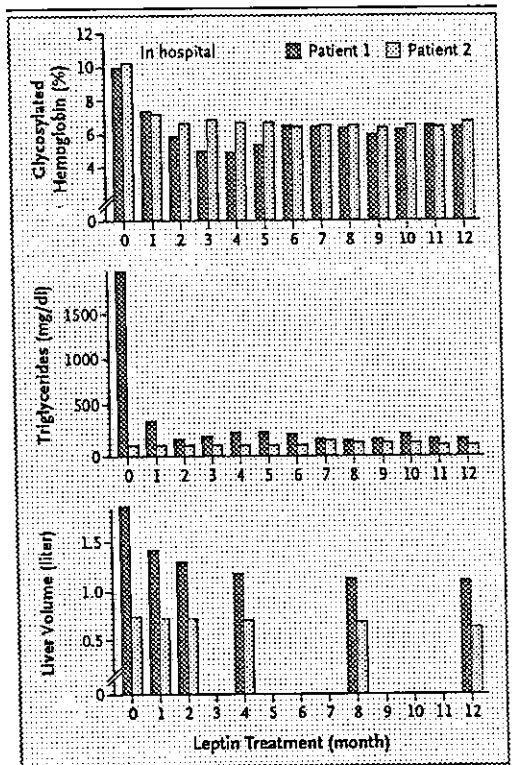

Figure 1. Glycosylated Hemoglobin Levels, Fasting Serum Triglyceride Levels, and Liver Volume in Patients 1 and 2 during 12 Months of Leptin-Replacement Therapy.
Liver volume was calculated with the use of computed tomographic imaging.

and plasma leptin concentrations (0.92 and 0.82 ng per milliliter, respectively). During leptin-replacement therapy, the serum leptin concentrations increased to 7.9 and 26.7 ng per milliliter at 4 months and 5.9 and 35.4 ng per milliliter at 12 months in Patients 1 and 2, respectively.

Both patients received leptin as inpatients for the first four months of therapy. After the initiation of leptin treatment, fasting plasma glucose levels normalized (208 mg per deciliter in Patient 1 and 142 mg per deciliter in Patient 2). Without the use of oral antidiabetic agents, the glucose levels in both patients were well controlled. The glycosylated hemoglobin levels were reduced to 4.8 percent and 6.5 percent, respectively, at four months and remained below 6.5 percent over a full year (Fig. 1). The elevated fasting triglyceride level and severe fatty liver in Patient 1 normalized (Fig. 1). During the year of treatment, we observed no adverse effects of leptin-replacement therapy and no skin reactions at the injection sites.

Our clinical trials in Japan show that leptin-replacement therapy is highly effective for a full year in patients with generalized lipodystrophy. Leptin-replacement therapy appears to be safe and effective for long-term treatment of lipoatrophic diabetes.

Ken Ebihara, M.D., Ph.D.
Hiroaki Masuzaki, M.D., Ph.D.
Kazuwa Nakao, M.D., Ph.D.
Kyoto University Graduate School of Medicine
Kyoto 606-8507, Japan
kebihara@kuhp.kyoto-u.ac.jp

1. Oral EA, Simha V, Ruiz E, et al. Leptin-replacement therapy for lipodystrophy. N Engl J Med 2002;346:570-8.

INSTRUCTIONS FOR LETTERS TO THE EDITOR

Letters to the Editor are considered for publication, subject to editing and abridgment, provided they do not contain material that has been submitted or published elsewhere. Please note the following: • Letters in reference to a *Journal* article must not exceed 175 words (excluding references), must be received within three weeks after publication of the article, and must be submitted over the Internet at http://authors.nejm.org. Letters not related to a *Journal* article must not exceed 400 words and may be submitted over the Internet or sent, typewritten and triple-spaced, by mail. • A letter can have no more than five references and one figure or table. • A letter can be signed by no more than three authors. • Financial associations or other possible conflicts of interest must be disclosed. (Such disclosures will be published with the letters. For authors of *Journal* articles who are responding to letters, this information appears in the original articles.) • Include your full mailing address, telephone number, fax number, and e-mail address with your letter.

Our address: **Letters to the Editor** • *New England Journal of Medicine* • 10 Shattuck St. • Boston, MA 02115

Our Web address: **http://authors.nejm.org**

Our fax numbers: **617-739-9864 and 617-734-4457**

We cannot acknowledge receipt of your letter, but we will notify you when we have made a decision about publication. Letters that do not adhere to these instructions will not be considered. Rejected letters and figures will not be returned. We are unable to provide prepublication proofs. Submission of a letter constitutes permission for the Massachusetts Medical Society, its licensees, and its assignees to use it in the *Journal*'s various print and electronic publications and in collections, revisions, and any other form or medium.

Diabetologia (2004) 47:47–54
DOI 10.1007/s00125-003-1272-8

Diabetologia

Reduction of diet-induced obesity in transgenic mice overexpressing uncoupling protein 3 in skeletal muscle

C. Son[1], K. Hosoda[1], K. Ishihara[2], L. Bevilacqua[3], H. Masuzaki[1], T. Fushiki[2], M. E. Harper[3, 4], K. Nakao[1]

[1] Department of Medicine and Clinical Science, Endocrinology and Metabolism, Kyoto University Graduate School of Medicine, Sakyo-ku, Kyoto 606-8507, Japan
[2] Division of Applied Life Sciences, Kyoto University Graduate School of Agriculture, Kyoto, Japan
[3] Department of Biochemistry, Microbiology and Immunology, Faculty of Medicine, University of Ottawa, Ontario, Canada
[4] Centre for Catalysis Research and Innovation, University of Ottawa, Ontario, Canada

Abstract

Aims/hypothesis. It has been suggested that uncoupling protein 3 (UCP3) can increase energy expenditure, thereby regulating body weight. Although studies on UCP3 knock-out mice suggest that lack of UCP3 function does not cause obesity or Type 2 diabetes, it is possible that up-regulation of UCP3 function improves these disorders or their clinical sequelae. A 10- to 20-fold increase of UCP3 gene expression is achievable through physiological or pharmacological stimuli. We examined the phenotype of transgenic mice with approximately 18-fold overexpression of mouse UCP3 mRNA in skeletal muscle.
Methods. We generated transgenic mice with approximately 18-fold overexpression of mouse UCP3 mRNA in skeletal muscle under control of the skeletal muscle-specific muscle creatine kinase gene promoter. The phenotype of these mice was analysed either on a standard diet or on a 4-week high-fat diet.
Results. In mice on standard chow, there was no difference in body weight, oxygen consumption and mitochondrial protonmotive force between transgenic mice and non-transgenic littermates. However, transgenic mice tended to have lower body weight, increased oxygen consumption and decreased mitochondrial protonmotive force than the control mice. Transgenic mice on a 4-week high-fat diet consumed much more oxygen and had noticeably less weight gain and less epididymal fat, as well as better glucose tolerance than non-transgenic littermates.
Conclusions/interpretation. Our study shows that 18-fold overexpression of UCP3 mRNA in the skeletal muscle reduced diet-induced obesity. An 18-fold increase of UCP3 mRNA can be attained by physiological or pharmacological stimuli, suggesting that UCP3 has therapeutic potential in the treatment of obesity. [Diabetologia (2004) 47:47–54]

Keywords Uncoupling protein 3 · skeletal muscle · transgenic mice · high-fat diet · obesity

Received: 23 June 2003 / Revised: 22 September 2003
Published online: 12 December 2003

Dr. K. Hosoda (✉), Department of Medicine and Clinical Science, Endocrinology and Metabolism, Kyoto University Graduate School of Medicine, 54 Shogoin Kawahara-cho, Sakyo-ku, Kyoto 606-8507, Japan
E-mail: kh@kuhp.kyoto-u.ac.jp
Abbreviations: UCP3, uncoupling protein 3; UCP2, uncoupling protein 2; UCP1, uncoupling protein 1; PPAR, peroxisome-proliferator-activated receptor; MCK, muscle creatine kinase; Δp, mitochondrial protonmotive force.

Uncoupling protein 3 (UCP3), which has been identified by several groups [1, 2, 3, 4], is reported to be involved in energy metabolism by uncoupling electron transport from ATP synthesis in mitochondria and is expressed at high levels in the skeletal muscle [3], an important organ in glucose and lipid metabolism [5]. Uncoupling protein 3 mRNA is expressed at much higher levels than uncoupling protein 2 (UCP2) mRNA in the skeletal muscle in vivo although accurate comparison is difficult [1, 2, 3, 4]. As uncoupling protein 1 (UCP1) gene expression is almost undetectable in the skeletal muscle [6], UCP3 is considered to be the most relevant UCP in the skeletal muscle. Several studies have reported that UCP3 gene expression

is up-regulated by triiodothyronine, catecholamines, fatty acids and peroxisome-proliferator-activated receptor (PPAR) agonists [4, 7, 8, 9].

It has been suggested that UCP3 is involved in energy expenditure, possibly leading to regulation of body weight. In two studies on UCP3 knock-out mice [10, 11] there was no difference between UCP3 knock-out and wild-type mice with regard to obesity, body temperature and serum concentrations of insulin, glucose, triglycerides and fatty acids. No obvious phenotype of UCP3 knock-out mice was observed when comparing their responses to fasting, exposure to cold, a high-fat diet and treatment with thyroid hormones with those of the control mice. This suggests that lack of UCP3 is not a major determinant of energy expenditure and obesity.

Although loss of the UCP3 function does not cause obesity or Type 2 diabetes, it is still possible that up-regulation of the UCP3 function improves these disorders. One study reported that glucose transport and GLUT4 translocation to the cell surface were increased in L6 myotubes in which UCP3 was overexpressed in vitro by adenovirus-mediated gene transfer [12]. Another study reported that transgenic mice overexpressing human UCP3 in the skeletal muscle weighed approximately 30% less than their wild-type littermates and that these transgenic mice were insulin-sensitive, with lower fasting plasma glucose and insulin concentrations [13]. These data suggest that drugs increasing UCP3 could have anti-obesity and/or antidiabetic effects. However, the levels of UCP3 overexpression in this study were very high (approximately 66-fold at the mRNA level), and no known stimulus will increase UCP3 gene expression by that amount. Several reports noted that UCP3 gene expression increased by a maximum of 10- to 20-fold in response to physiological or pharmacological stimuli in vivo [14]. We have reported that an agonist for PPARδ increased UCP3 gene expression by approximately 20-fold using L6 myotubes in vitro [15]. In this context we produced transgenic mice that overexpress mouse UCP3 mRNA in the skeletal muscle by approximately 18-fold. Furthermore, to explain the effect of the increased UCP3 on diet-induced obesity, we examined the phenotype of transgenic mice on high-fat diet.

Materials and methods

Generation of transgenic mice overexpressing UCP3. Based on the non-coding sequence of rat UCP3 cDNA [3], sense and antisense primers (sense: 5′-CAA AGG AAC CAG GCC ATC CTC CGG AAC C-3′; antisense: 5′-AA AGT ACC AAG CGG CCT GCT TGC CTT GT-3′) were prepared. Reverse transcription-PCR was done using Superscript (Invitrogen, Carlsbad, Calif., USA) with 10 μg of total RNA from mouse gastrocnemius muscle [16]. The PCR products were subcloned and sequenced (Accession ID: AB008216) by the dideoxy method [3]. A fusion gene comprising the mouse muscle creatine kinase (MCK) promoter and mouse UCP3 cDNA coding sequences was designed to enable UCP3 expression to be targeted mainly to the skeletal muscle (Fig. 1a) [17]. The purified *Hind* III-*Sac* I fragment (10 μg/ml) was microinjected into the pronucleus of fertilised BDF 1 (DBA2 X C57/B6) mouse eggs (Japan SLC, Hamamatsu, Japan). The viable eggs were transferred into the oviducts of pseudopregnant female ICR mice (Japan CLEA, Osaka, Japan) using standard techniques [18]. Transgenic founder mice were identified by Southern blot analysis of tail DNAs using the mouse UCP3 cDNA fragment as a probe [18]. Transgenic mice were used as heterozygotes. Transgenic mice were back-crossed with C57/B6 mice. Mice of F4 generation or later were used in this study. Animals were housed in a temperature-, humidity-, and light-controlled room (temperature: 22±0.5°C, humidity: 50%, 12-h light, 12-h darkness) with free access to water and food. All experimental procedures were approved by the Kyoto University Graduate School of Medicine Committee on Animal Research and carried out in accordance with the Declaration of Helsinki as revised in 2000. The principles of laboratory animal care (NIH publication no. 85-23, revised 1985); were followed, as well as any specific national laws.

RNA extraction and northern blot analysis. Total RNA was extracted from tissues using Trizol reagent (Invitrogen) as described previously [19]. Filters containing 30 μg of total RNA were prepared. Northern blot analyses were done using cDNA probes of mouse UCP3 [9]. The density of 18S rRNA stained with ethidium bromide was used to monitor the amount of total RNA in each sample.

Western blot analysis. The gastrocnemius muscle was removed and homogenised in ice-cold buffer (50 mmol/l Tris (pH 7.4), 150 mmol/l NaCl, 1% Triton X-100, 1% sodium deoxycholate, and 0.1% SDS) containing 1 mmol/l phenylmethlysulfonyl fluoride, 0.01 mmol/l leupeptin and 5 μg/ml aprotinin. Homogenates were centrifuged and supernatants were used for analysis of total protein. Mitochondrial fraction was obtained from gastrocnemius muscle as described previously [20]. Antibody for rat UCP3, its inhibitory peptide and antibody for human UCP3 were purchased from Alpha Diagnostic International (San Antonio, Tex., USA). Total and mitochondrial protein were used for SDS-PAGE and western blot analyses using antibodies for rat UCP3 or human UCP3 [21].

Isolation of mitochondria. Mitochondria were isolated from gastrocnemius skeletal muscle (n=7) as described previously [22, 23]. Mice were decapitated before removal of skeletal muscle. The skeletal muscle was homogenised in buffer containing 250 mmol/l sucrose, 1 mmol/l HEPES and 0.2 mmol/l EDTA (pH 7.2 with KOH). Fractionation of the homogenate was achieved by spinning for 10 min at 1500 g and at 4°C. The supernatant was then poured through a 250 μmol/l Nitex screen (Dynamic Aqua-Supply, British Columbia, Canada) and re-spun for 14 min at 16 000 g and at 4 C to obtain a mitochondrial pellet. The pellet was re-suspended on ice in 175 μl of suspension medium containing 120 mmol/l KCl, 20 mmol/l sucrose, 3 mmol/l HEPES, 2 mmol/l $MgCl_2$, 2 mmol/l EGTA and 0.5% BSA (pH 7.2 with KOH). Stock 9% BSA was defatted by the Chen method [24] and dialysed against 153 mmol/l NaCl and 11 mmol/l KCl. The protein concentration of the mitochondrial suspension was assayed by the modified Lowry method using BSA as the reference standard.

Measurement of mitochondrial oxygen consumption and mitochondrial protonmotive force (Δp). Mitochondrial suspensions

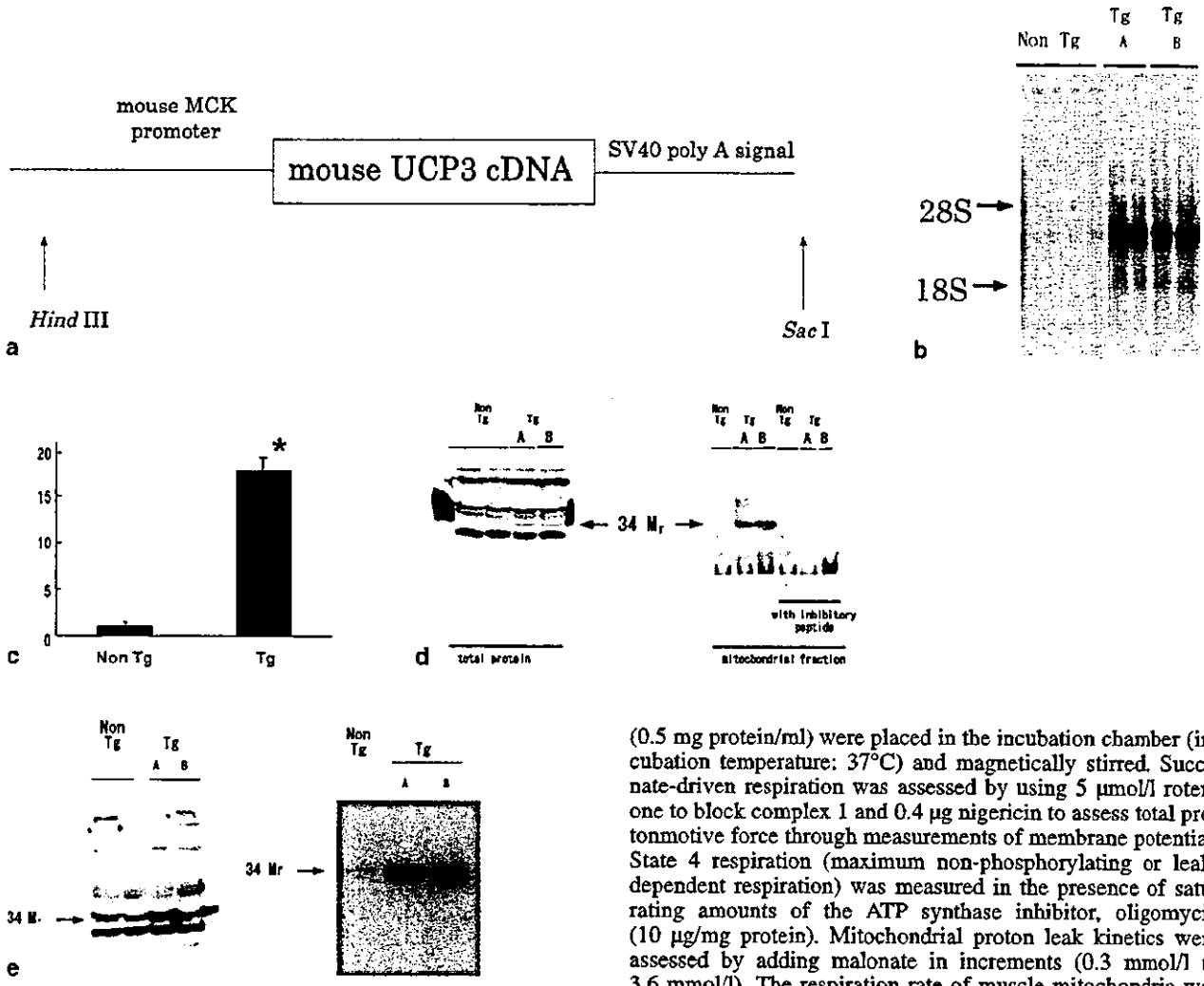

Fig. 1a–e. Generation of transgenic mice overexpressing UCP3. Schematic representation (**a**) of the mouse creatine kinase promoter and mouse UCP3 fusion gene. The coding region of mouse UCP3 cDNA is denoted by the closed box. Northern blot analysis (**b**) of transgene expression in the gastrocnemius muscle from 8-week-old transgenic mice of Line A and Line B, and UCP3 mRNA expression in the gastrocnemius muscle from 8-week-old non-transgenic littermates. Total RNA analysed: 30 μg. Tg, transgenic mice; non Tg, non-transgenic littermates. The bar graph (**c**) shows quantitative analysis of UCP3 mRNA expression. Levels of UCP3 mRNA expression increased approximately 18-fold in transgenic mice Line A in comparison with the non-transgenic littermates. Data are expressed as means ± SE (n=5). Western blot analysis (**d**) using antirat UCP3 antibody. Amounts analysed were: 100 μg of total protein and 600 ng of protein from mitochondrial fraction. No added peptide or inhibitory peptide (to which the antibody was raised) was included during the first antibody incubation. Western blot analysis (**e**) using human UCP3 antibody. Amounts analysed were: 100 μg of total protein and 600 ng of protein from mitochondrial fraction

(0.5 mg protein/ml) were placed in the incubation chamber (incubation temperature: 37°C) and magnetically stirred. Succinate-driven respiration was assessed by using 5 μmol/l rotenone to block complex 1 and 0.4 μg nigericin to assess total protonmotive force through measurements of membrane potential. State 4 respiration (maximum non-phosphorylating or leak-dependent respiration) was measured in the presence of saturating amounts of the ATP synthase inhibitor, oligomycin (10 μg/mg protein). Mitochondrial proton leak kinetics were assessed by adding malonate in increments (0.3 mmol/l to 3.6 mmol/l). The respiration rate of muscle mitochondria was measured using a Clark-type oxygen electrode (Hansatech, Norfolk, UK) [22]. Protonmotive force was measured using a methyltriphenylphosphonium-sensitive electrode as described previously [22].

Measurements of body weight and cumulative food intake. Body weight was measured daily, beginning at 4 weeks of age. Food intake was measured daily over a 1-week period at the age of 26 weeks. It was measured in male mice, which were maintained in individual metabolic cages.

Measurement of oxygen consumption. The gas analyser used to assess the metabolic rate consisted of six acrylic metabolic chambers, CO_2 and O_2 analysers (RL-600, AlcoSystem, Tokyo, Japan), and a switching system (ANI6-A-S, AlcoSystem) to sample gas from each metabolic chamber. Each metabolic chamber had 125.4 cm^2 floor space and was 6.5 cm in height. Oxygen consumption was calculated by measuring the O_2 and CO_2 concentrations of each chamber [25].

Glucose and insulin tolerance tests. For the glucose tolerance test 20-week-old transgenic mice and their non-transgenic littermates were treated with an intraperitoneal injection of 2.0 mg/g glucose after an overnight fast [18]. For the insulin tolerance test, mice were injected intraperitoneally with 0.5 mU/g human regular insulin (Novolin R, Novo Nordisk, Bagsvard, Denmark) [18]. Blood samples were taken from the

mouse tail vein before and 30, 60 and 90 min after the injection. Plasma glucose concentrations were measured by the glucose oxidase method with a reflectance glucometer (One Touch II, Lifescan, Milpitas, Calif., USA).

High-fat diet study. To examine the effect of UCP3 overexpression on diet-induced obesity, UCP3 transgenic mice and non-transgenic littermates were fed a high-fat diet for 4 weeks from 24 weeks of age. The high-fat diet was produced by Oriental Bioservice (Kyoto, Japan) [26]. Its fat content was 23%, whereas that of standard chow was 7%.

Histology. We did histological examinations of skeletal muscle, white and brown adipose tissues, heart, liver, and pancreas. This was done by light microscopy, using 5-μm-thick sections from 10% buffered, formalin-fixed, paraffin-embedded specimens which were stained with hematoxylin and eosin [18].

Measurement of plasma concentrations of glucose, triglyceride, fatty acids, cholesterol and insulin. Blood samples were taken from the retro-orbital sinus of mice at 9:00 hours after overnight fasting or at 14:00 hours. Plasma glucose, triglyceride, and insulin concentrations were measured by the glucose oxidase method with a reflectance glucometer, the enzymatic kit (Wako Pure Chemical, Osaka, Japan) and by RIA with mouse insulin standards (Morinaga BioLab, Yokohama, Japan), respectively [18].

Statistical analysis. Data were expressed as means ± SE. Statistical significance was tested by one-way ANOVA. If F was found to be significant, the Student's t test was used to test individual differences. A p value of less than 0.05 was considered statistically significant.

Results

Generation of transgenic mice overexpressing UCP3. A fusion gene comprising the mouse MCK promoter and mouse UCP3 cDNA coding sequence was designed to enable UCP3 expression to be targeted to the skeletal muscle (Fig. 1a). Several transgenic lines with different copy numbers of the transgene were obtained. With the mouse UCP3 cDNA probe, northern blot analysis showed that an mRNA species of 2.4 kb in size, which was expected from the fusion gene of MCK promoter and mouse UCP3 cDNA, was expressed abundantly in the skeletal muscle from several lines of the transgenic mice (Fig. 1b). The highest UCP3 mRNA levels were obtained in Line A of the transgenic lines and were approximately 18-fold higher than in non-transgenic littermates (Fig. 1b,c). The second highest mRNA levels were approximately 15-fold higher (Line B; Fig. 1b).

Western blot analysis of protein expression in the skeletal muscle of these two lines detected multiple bands, separated by electrophoresis, of total protein extracted from the skeletal muscle (Fig. 1d). When protein of mitochondrial fraction was electrophoresed, antirat UCP3 antibody detected, as expected from the molecular mass of mouse UCP3, a single band near 34 M_r (Fig. 1d). This band at 34 M_r disappeared when

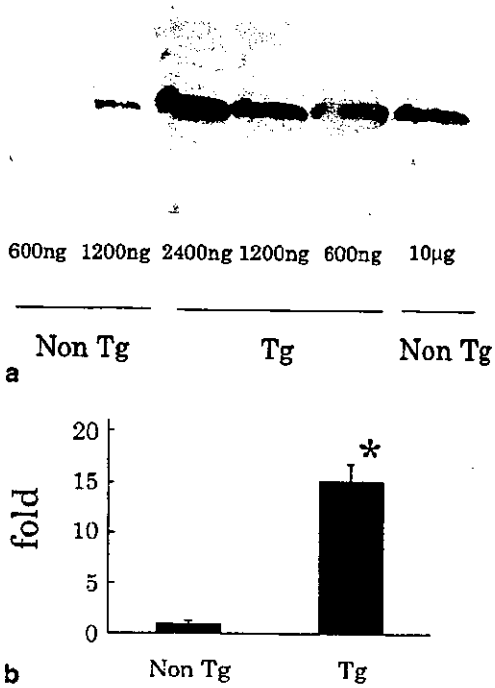

Fig. 2a, b. Quantification of UCP3 protein in mitochondria from skeletal muscle of transgenic mice. Representative result of western blot analysis (**a**) using antirat UCP3 antibody. Line A transgenic mice were examined. Various amounts of protein from mitochondria were analysed. The density of bands of 600 ng of protein from UCP3 transgenic mice was nearly equal to that of 10 μg of protein from non-transgenic littermates. The bar graph (**b**) shows quantitative analysis of UCP3 protein, which increased approximately 15-fold in transgenic mice as compared with non-transgenic littermates. Data are expressed as means ± SE (n=5)

inhibitory peptide was simultaneously incubated (Fig. 1d). Similar results were obtained using anti-human UCP3 antibody (Fig. 1e).

To quantify UCP3 concentrations in the skeletal muscle of transgenic mice, we examined transgenic mice of Line A. Western blot analyses were done using various amounts of protein from skeletal muscle mitochondria. Figure 2a is a representative result. It shows that the density of bands of 600 ng of protein from a UCP3 transgenic mouse was nearly equivalent to that of 10 μg of protein from a non-transgenic littermate. UCP3 protein was approximately 15 times higher in transgenic mice than in nontrasgenic littermates (n=5; Fig. 2b). As the MCK promoter also induces gene expression in the cardiac muscle, we examined the UCP3 gene expression there, finding that UCP3 mRNA levels were slightly higher in the cardiac muscle of Line A and Line B than in those of non-transgenic littermates. In Line A and Line B, UCP3 mRNA levels in the cardiac muscle were less than 1% of those in the skeletal muscle. UCP3 protein levels were not detected in the cardiac muscle either of

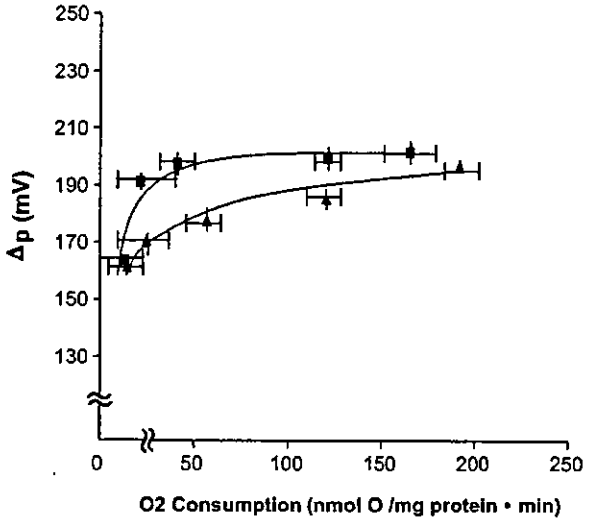

Fig. 3. Kinetic response of the proton leak to protonmotive force in mitochondria isolated from hindlimb muscle of UCP3 transgenic mice (▲) and non-transgenic littermates (■) (n=7, each). State 4 respiration was established using a saturating concentration of oligomycin (10 μg/mg protein). Subsequent additions of malonate (0.3 mmol/l to 3.6 mmol/l) provided the overall kinetics of the proton leak reactions. Data are expressed as means ± SE. Statistical significance was determined by Student's t test. A p value of less than 0.05 was considered statistically significant

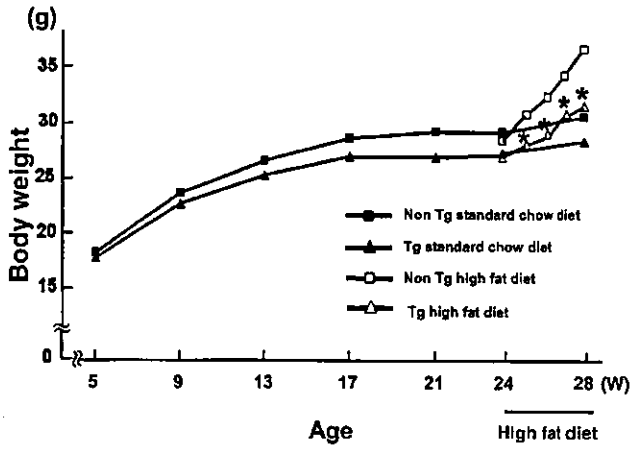

Fig. 4. Changes in body weight of male transgenic mice and non-transgenic littermates on standard chow and on high-fat diets. UCP3 transgenic mice and non-transgenic littermates were fed a standard chow diet for the first 24 weeks (n=22 to 25). For the following 4 weeks, some were fed a high-fat diet (n=7 to 9), while others continued on the standard chow diet (n=16 to 17). Data are expressed as means ± SE. *p<0.05 vs non-transgenic littermates on high-fat diet

transgenic mice or of non-transgenic littermates. UCP3 mRNA levels in the brown adipose tissue of transgenic mice were not significantly different from those of non-transgenic littermates (107±12% in Line A and 112±9% in Line B, p>0.05). Northern blot analysis with 30 μg of total RNA failed to detect any band of UCP3 mRNA in tissues of transgenic mice other than skeletal muscle, cardiac muscle and brown adipose tissue. The transgenic mice of both lines were fertile, and viable throughout adulthood with no appreciable complications. All these results were observed in transgenic mice of each sex.

Mitochondrial proton leak. The kinetic response curve for the proton leak reactions showed trends towards increased mitochondrial oxygen consumption over a range of values for Δp (Fig. 3). The absolute values for oxygen consumption and Δp at State 4 (the point on each curve at the furthermost point on the right) were not statistically different between groups (Fig. 3). However, UCP3 transgenic mice tended to have higher State 4 oxygen consumption than the non-transgenic littermates (202.9±10.1 nmol O_2 mg^{-1} min^{-1} vs 193.1±7.1 nmol O_2 mg^{-1} min^{-1}, p=0.3). UCP3 transgenic mice also tended to have a lower State 4 Δp value (196.5±2.2 mV for transgenic mice vs 201.3± 4.1 mV for non-transgenic littermates, p=0.2).

Phenotype of UCP3 transgenic mice on standard chow diet. In transgenic mice and non-transgenic littermates on a standard chow diet no significant difference in body weight was observed, although the transgenic mice tended to be lighter (27.6±0.6 g vs 29.9±0.6 g at 21 weeks, p=0.07; Fig. 4). No differences in food intake (2.8±0.1 g/day vs 2.7±0.1 g/day, p>0.05), oxygen consumption (46.1±2.6 ml kg^{-1} min^{-1} vs 41.3±1.1 ml kg^{-1} min^{-1}, p>0.05), rectal temperature (36.1±0.6 C vs 35.9±0.5°C, p>0.05) and histological analysis were observed between transgenic and non-transgenic littermates. No significant differences were noted in serum concentrations of glucose, insulin, cholesterol, triglyceride and fatty acids, although these tended to be lower in transgenic mice than in non-transgenic littermates (Table 1). In glucose and insulin tolerance tests on 28-week-old transgenic mice and non-transgenic littermates no significant differences were noted (Fig. 5a, Fig. 6a). As the phenotype described above was noted in transgenic mice of Line A and Line B, we used Line A, the line expressing the highest levels of UCP3, for further examination.

Body weight of transgenic mice on high-fat diet. One week after beginning the high-fat diet, the transgenic mice were approximately 10% less obese than the non-transgenic littermates (28.3±0.6 g vs 31.6±0.8 g, p<0.05; Fig. 4). After 4 weeks of a high-fat diet, the transgenic mice were approximately 14% less obese than the non-transgenic littermates (32.4±1.3 g vs 37.5±1.3 g, p<0.05; Fig. 4). Body weight gain for this 4-week period was nearly 49% less in transgenic mice than in non-transgenic littermates (4.4±1.1 g vs 8.6±0.8 g, p<0.05). The weight of the epidydimal fat pad was approximately 20% lower in transgenic mice than in non-transgenic littermates after the 4-week